DARN/SUPERDARN

A Global View of the Dynamics of High-Latitude Convection

R. A. GREENWALD[1], K. B. BAKER[1], J. R. DUDENEY[2], M. PINNOCK[2], T. B. JONES[3], E. C. THOMAS[3], J.-P. VILLAIN[4], J.-C. CERISIER[5], C. SENIOR[5], C. HANUISE[6], R. D. HUNSUCKER[7], G. SOFKO[8], J. KOEHLER[8], E. NIELSEN[9], R. PELLINEN[10], A. D. M. WALKER[11], N. SATO[12] and H. YAMAGISHI[12]

[1] *The Johns Hopkins University, Applied Physics Laboratory Laurel, Maryland, USA;*
[2] *British Antarctic Survey, Natural Environment Research Council Cambridge, England;*
[3] *Department of Physics, Leicester University Leicester, England;*
[4] *Laboratoire de Physique et Chimie de l'Environnement Centre National de la Recherche Scientifique, Orléans, France;*
[5] *Centre d'Etude des Environnement Terrestre et Planétaires Centre National de la Recherche Scientifique, Saint Maur, France;*
[6] *Laboratoire de Sondages Electromagnetiques de l'Environnement Terrestre Centre National de la Recherche Scientifique, Toulon, France;*
[7] *Geophysical Institute, University of Alaska Fairbanks, Alaska, USA;*
[8] *Department of Physics, University of Saskatchewan Saskatoon, Saskatchewan, Canada;*
[9] *Max Planck Institut für Aeronomy Lindau am Harz, Germany;*
[10] *Finnish Meteorlogical Institute Helsinki, Finland;*
[11] *University of Natal Durban, Republic of South Africa;*
[12] *National Institute of Polar Research Tokyo, Japan*

(Received 6 July, 1993)

Abstract. The Dual Auroral Radar Network (DARN) is a global-scale network of HF and VHF radars capable of sensing backscatter from ionospheric irregularities in the E and F-regions of the high-latitude ionosphere. Currently, the network consists of the STARE VHF radar system in northern Scandinavia, a northern-hemisphere, longitudinal chain of HF radars that is funded to extend from Saskatoon, Canada to central Finland, and a southern-hemisphere chain that is funded to include Halley Station, SANAE and Syowa Station in Antarctica. When all of the HF radars have been completed they will operate in pairs with common viewing areas so that the Doppler information contained in the backscattered signals may be combined to yield maps of high-latitude plasma convection and the convection electric field. In this paper, the evolution of DARN and particularly the development of its SuperDARN HF radar element is discussed. The DARN/SuperDARN network is particularly suited to studies of large-scale dynamical processes in the magnetosphere-ionosphere system, such as the evolution of the global configuration of the convection electric field under changing IMF conditions and the development and global extent of large-scale MHD waves in the magnetosphere-ionosphere cavity. A description of the HF radars within SuperDARN is given along with an overview of their existing and intended locations, intended start of operations, Principal Investigators, and sponsoring agencies. Finally, the operation of the DARN experiment within ISTP/GGS, the availability of data, and the form and availability of the Key Parameter files is discussed.

1. Introduction

One of the primary goals of the ISTP/GGS mission is to study the transport of mass and energy through the Geospace environment. The solar wind plasma imping-

Space Science Reviews **71:** 761–796, 1995.

ing upon the Earth's magnetosphere directly or indirectly excites a wide range of processes which lead to such phenomena as high-latitude auroras, plasma convection, electrojet currents, geomagnetic storms and substorms, and disturbances of the upper atmosphere extending from the polar regions to the tropics. In order to understand these processes, especially those with very large spatial dimension, a global view is required. The satellites of the ISTP/GGS mission provide this global view by putting similar instruments in different parts of the magnetosphere and in the solar wind. The GEOTAIL satellite is in a near-equatorial orbit that extends to very large distances in the Earth's magnetotail. Generally, it is located on magnetic field lines that map into the very high-latitude, nightside polar ionosphere, but for shorter periods, it can be located at or near the dayside magnetopause and map into the high-latitude dayside ionosphere. The POLAR satellite will have a near-polar orbit passing over the auroral zones and polar cap and the WIND satellite will be located at the L-1 Lagrangian point to provide information on the input conditions of the solar wind. To set the measurements into a global context, the POLAR satellite will include auroral imaging cameras at ultraviolet and visible wavelengths to provide dynamic and global views of the auroral precipitation process and the global distribution of high-latitude ionospheric conductivity. Additional global-scale information will be provided by the ground-based instruments contributing to the ISTP/GGS project. A subset of these is the Dual Auroral Radar Network (DARN) which is a ground-based array of HF and VHF coherent-backscatter radars that have the unique capability of providing global-scale observations of the structure and dynamics of plasma convection and electric fields in the auroral zones and polar caps.

In order to fully appreciate the potential contribution of DARN to the ISTP/GGS mission, it is necessary to understand the nature of coherent scatter and the contributions that coherent scatter radars have made to ionospheric and magnetospheric physics over the past two decades.

1.1. Nature of Coherent Backscatter

Coherent-scatter radars are sensitive to Bragg scattering from small-scale electron density irregularities in the ionosphere. In the case of backscatter, a given radar is sensitive to ionospheric irregularities having a wavelength equal to one-half of the radar wavelength. Since coherent-scatter radar observations have historically been performed at VHF (30–300MHz) and UHF (300–3000 MHz) frequencies, most radar research prior to the 1980s has been limited to irregularity wavelengths ranging from ~20 cm to ~3 m.

Ionospheric irregularities are noted for their magnetic field-aligned structure. That is, their wavenumber vector is directed very nearly orthogonal to the magnetic field. The practical consequence of this physical attribute is that the incident radar signal must also be orthognal to the magnetic field in order for the scattered signal to return to the radar. This condition poses certain geometrical constraints on the iono-

spheric regions that can be sensed with coherent scatter radars. In particular, when coherent VHF and UHF radars are used at high latitudes where the the magnetic field lines are nearly vertical, it becomes impossible to achieve the orthogonality condition above E-region altitudes (90–130 km). Consequently, all historical studies of high-latitude coherent backscatter were of E-region irregularities.

Past research has shown that most ionospheric electron-density structure is produced by plasma instability processes (e.g. review by Fejer and Kelley, 1980). In the E-region, plasma streaming instabilities, most notably the cross-field two-stream (Buneman, 1963; Farley, 1963) and gradient drift (e.g. Knox, 1964; Reid, 1968) instabilities, are of particular importance. The streaming nature of these instabilities causes them to collocate with ionospheric electrojets and to be observed predominantly near the equator and at high latitudes. In fact, radar backscatter has been shown to be a useful technique for locating the auroral electrojet currents (Greenwald *et al.*, 1975). Another E-region instability which has been proposed and potentially identified is the electrostatic ion cyclotron instability (Fejer *et al.*, 1984). The importance of this instability is open to debate. If it is observed, it is only required to explain a small fraction of the observations.

The F-region (above 150 km) of the ionosphere also contains a wealth of electron density irregularities. These irregularities, too, are produced by plasma instability processes and, at high latitudes where the irregularities are especially abundant (Aarons, 1973), they may also be formed by structured particle precipitation and images of magnetospheric turbulence. The most common plasma instability is an F-region form of the gradient drift instability (Simon, 1963). In addition, the Rayleigh-Taylor (Dungey, 1956), Kelvin-Helmholtz (e.g. Keskinen *et al.*, 1988), and Current Convective (Ossakow and Chaturvedi, 1979) Instabilities are also believed to be fairly active.

Historically, most radar studies of F-region irregularities have been confined to low and mid-latitudes where VHF or UHF radars can achieve the requisite orthogonality condition with the Earth's magnetic field (e.g., Woodman and La Hoz, 1976; Tsunoda *et al.*, 1979). Under the aforementioned Bragg scattering condition, the wavelength range investigated were generally shorter than 3 m. During the past decade, HF (3–30 MHz) radars have been used increasingly to study F-region irregularities in the high-latitude ionosphere. These radars use ionospheric refraction to achieve the orthogonality condition in both the E and F-regions. They also extend the wavelength range of irregularity investigations out to 19 m, thereby bringing the observations into a regime where plasma fluid effects dominate over plasma kinetic effects.

1.2. Brief History of Convection Studies with Coherent Radars

The first extensive use of coherent scatter radars to study ionospheric convection took place in the late 1970s with the development of the Scandinavian Twin Auroral Radar Experiment (STARE) in northern Scandinavia (Greenwald *et al.*, 1978).

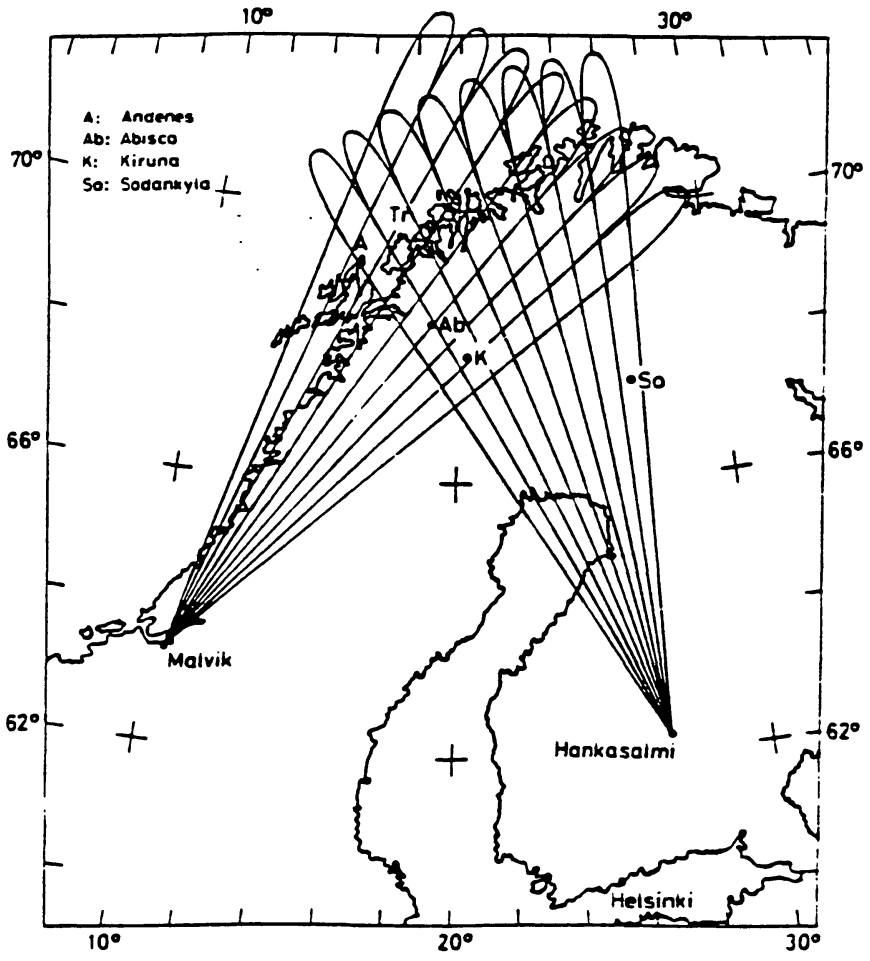

Fig. 1. Map of Scandinavia in geographic coordinates showing the eight overlapping beams of the STARE radars (From Greenwald *et al.*, 1978).

STARE consists of two pulsed bistatic phased-array radars located in Malvik, Norway and Hankasalmi, Finland. The radars are directed over a large common viewing area (approximately 400 × 400 km) centered on northern Scandinavia as indicated in Figure 1. Within this area the radars are capable of sensing with good spatial and temporal resolution the intensity and Doppler velocity of E-region ionospheric irregularities. The Doppler data from the two radars are combined to determine the vector velocity of the irregularities with 20 × 20 km spatial and 20 s temporal resolution. Subsequent comparisons with rocket double-probe data (Cahill *et al.*, 1978) indicated that the irregularity drifts could be related to ionospheric plasma drifts, a result that led to the STARE system being used extensively for studies of the two-dimensional structure and dynamics of ionospheric plasma convection. At that time, it appeared to be the only instrument capable of providing two-dimensional images of the structure of ionospheric convection patterns.

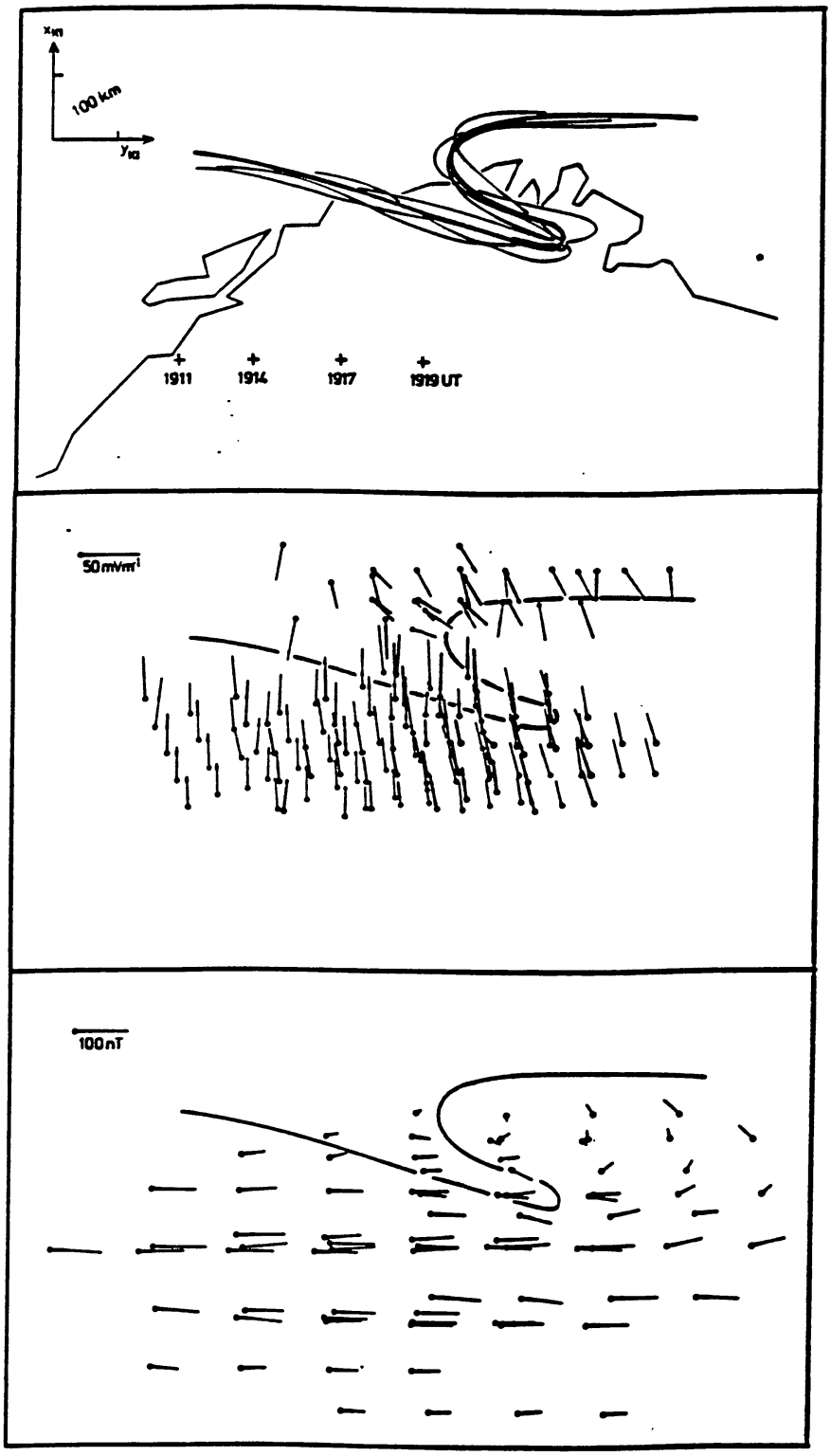

Fig. 2. Superimposed epoch analysis of the spatial distribution of auroral luminosity (upper panel), electric field vectors (middle panel), and equivalent currents (lower panel) during the passage of a westward traveling surge at approximately 1911 UT on March 27, 1977. The + signs in the upper panel represent the relative position of the all-sky camera to the surge at the indicated times (From Inhester *et al.*, 1981).

During the International Magnetospheric Study (IMS), the STARE radars were extensively used in coordination with the Scandinavian magnetometer network (Kueppers *et al.*, 1979), the all sky cameras of the Finnish Meteorlogical Institute, and other ground-based instrumentation to study the electrodynamic behavior of a wide range of auroral-zone phenomena. A few of the many accomplishments of this instrument cluster included the identification of the electromagnetic structure of Pc5 hydromagnetic resonances in the high-latitude ionosphere (e.g. Walker *et al.*, 1979), the determination of plasma convection patterns and currents in the vicinity of the Harang Discontinuity (Nielsen and Greenwald, 1979; Kunkel *et al.*, 1986), and the determination of currents and electric fields associated with the passage of a westward traveling surge (Inhester *et al.*, 1981). An example of how these data were assimulated in the study of the westward traveling surge is shown in Figure 2. Here, the upper panel shows a superposition of four epochs of the auroral luminosity from the surge as it passed over northern Scandinavia, while the middle and lower panels show the electric fields obtained from STARE and the equivalent currents obtained from the Scandinavian magnetometer array. Detailed optical, magnetic, and radar images such as this had never been achieved with any other instrument cluster.

The success of the STARE research effort led to the development of several additional paired VHF radar systems. These included the Sweden And Britain Radar Experiment (SABRE) (Nielsen *et al.*, 1983) and the Bistatic Auroral Radar System (BARS) (McNamara *et al.*, 1983). Both of these systems were identified as elements of the DARN network.

During the 1980s, a number of coordinated studies between STARE and the European Incoherent Scatter Radar (EISCAT) revealed some shortcomings of the use of E-region coherent backscatter for the measurement of plasma convection and ionospheric electric fields. Specifically, it was found that STARE often detected two-stream irregularities that move at the ion acoustic velocity even though the line-of-sight electric drift velocity may be significantly larger. This causes the electron (plasma) drift speeds estimated from the E-region coherent scatter technique to be lower than the plasma drift speeds determined with incoherent scatter radars (Nielsen and Schlegel, 1983). These studies showed, however, that the errors introduced by this velocity saturation did not seem to have a significant effect on the determination of the plasma drift direction (Nielsen and Schlegel, 1983).

For very large electric fields the ion acoustic velocity is enhanced due to electron heating caused by the plasma turbulence associated with the instabilities. Nielsen and Schlegel (1985) have attempted to use this characteristic to determine an empirical relationship between the ion acoustic velocity and the E-region electron drift velocity. Using this relationship, they have reanalyzed 38 hours of common STARE-EISCAT observations and, as indicated in Figure 3, obtained reasonably good agreement between the two sets of measurements in both magnitude and direction. Nevertheless, there are still residual questions on the general validity

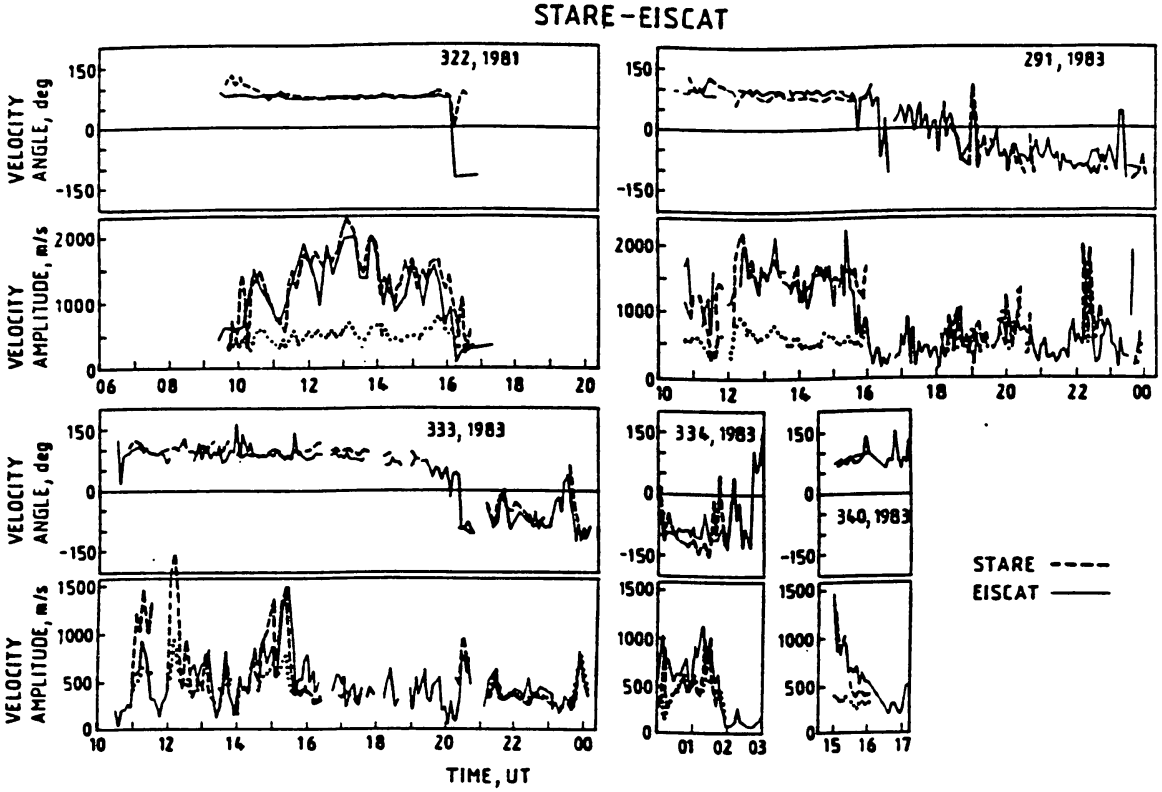

Fig. 3. Thirty-eight hours of STARE-EISCAT drift velocity comparisons. EISCAT velocities are indicated by solid lines. STARE velocities with speed determined from ion-acoustic relationship are indicated by dashed curves. STARE speeds determined directly from Doppler projections are indicated by dotted lines (From Nielsen and Schlegel, 1985).

deriving plasma motions from E-region backscatter data as evidenced by recent papers by Haldoupis *et al.* (1993) and Robinson (1993).

The Nielsen and Schlegel (1985) results shown in Figure 3 also indicate that fairly substantial E-region electron drift velocities are generally required for E-region coherent backscatter to be observed. Careful examination of this data set as well as data sets of other researchers indicate that an electron drift velocity of approximately 300–400 m/s is often required for the irregularities to be formed. This is equivalent to an ionospheric electric field of ~15–20 mV/m.

As the limitations of the E-region coherent scatter technique were becoming clearer and the ISTP/GGS mission was evolving into its current form, a new approach to coherent backscatter utilizing radars operating at HF frequencies was being developed in France, the U.S., and Britain. At these lower frequencies ionospheric refraction allows the orthogonality condition to be satisfied in both the E and F-region of the ionosphere as illustrated in Figure 4. The figure illustrates that the nearly vertical magnetic field lines at high latitudes lead to non-orthogonal scattering at VHF and higher frequencies with the scattered signals propagating into space. In contrast, the refraction which occurs at HF causes the radar signals to

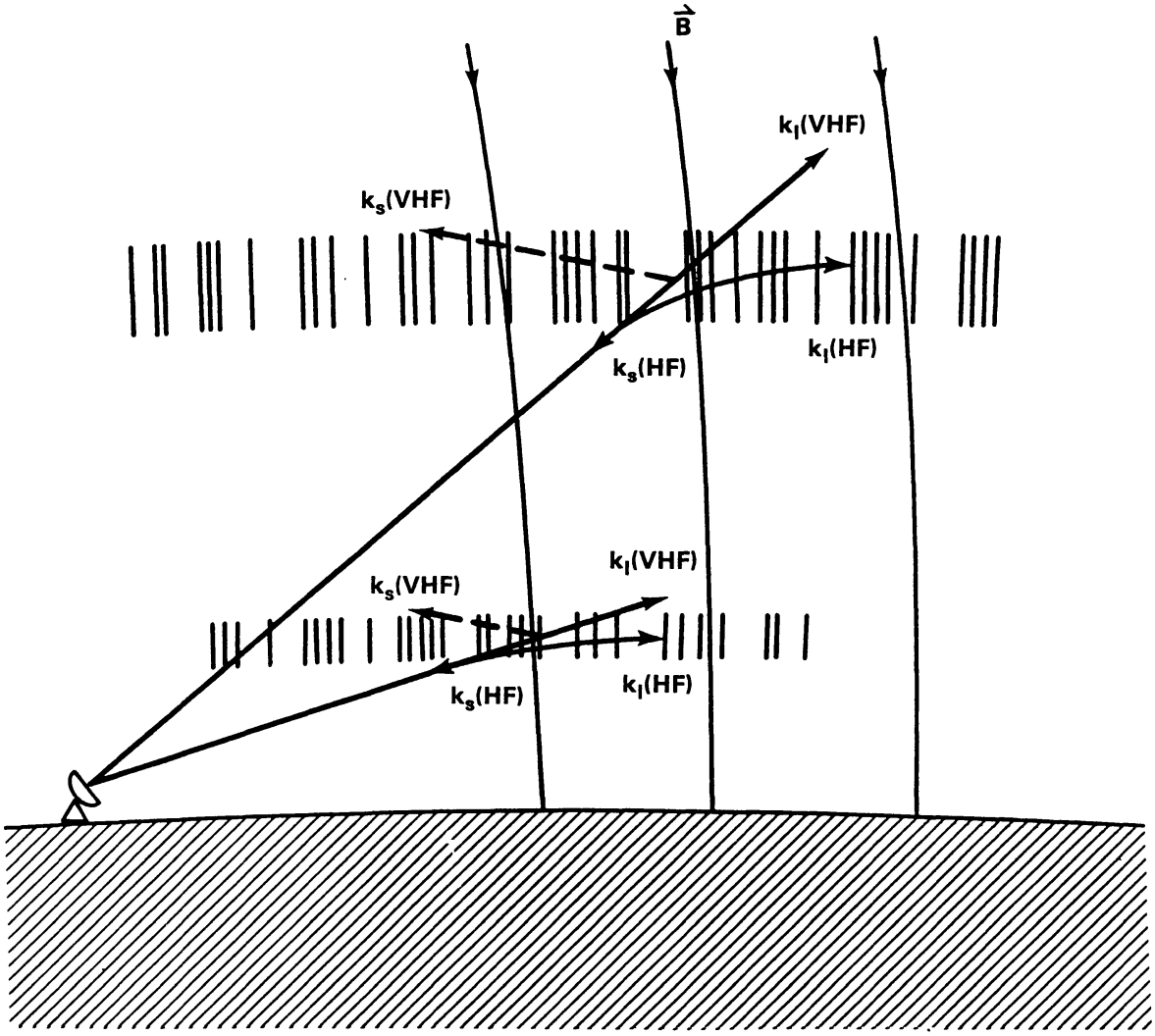

Fig. 4. Illustration of manner in which VHF and higher frequencies are scattered into space by high-latitude electron density irregularities. HF signals are refracted toward the horizontal as they enter the ionospheric layers. If the signals are propagating perpendicular to the magnetic field when they encounter regions of ionospheric irregulaties, the backscattered signals will return to the radar.

become orthogonal to the magnetic field lines. If there were ionospheric irregularities in these regions, they would backscatter the radar signals which would return to the radar site.

It is important to note that except for limited regions of intense auroral precipitation, the F-region electron density is generally much greater than the electron density in the underlying E-region. Consequently, the requisite refraction occurs predominantly in the F-layer over a broad range of altitude extending throughout the bottomside and into the topside of the ionosphere. Ionospheric irregularities produced by F-region plasma instabilities, particle precipitation, or images of magnetospheric turbulence may exist throughout this altitude range.

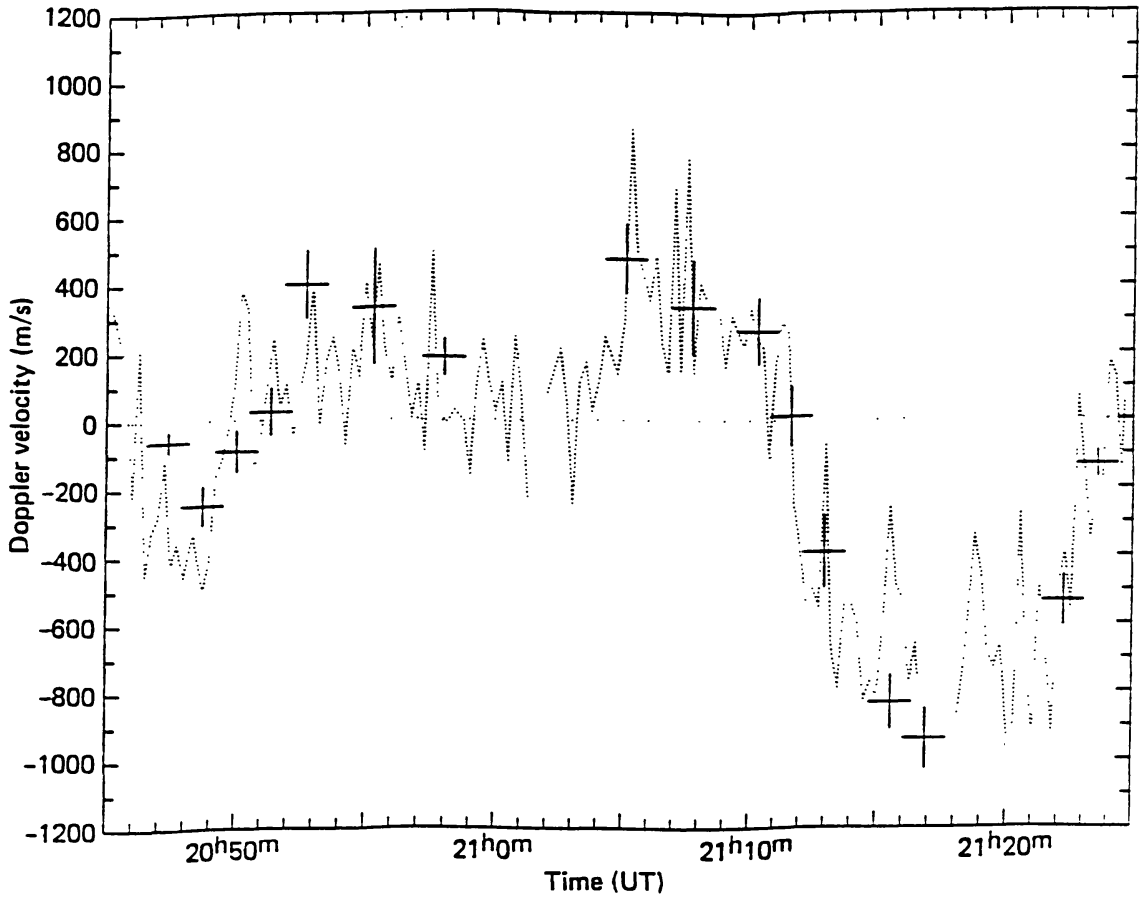

Fig. 5. Comparison of F-region Doppler velocities observed with the Sondrestom incoherent scatter radar and the Goose Bay coherent scatter radar. The Sondrestrom observations are indicated by the dotted lines and the Goose Bay observations by the crosses. See text for fuller description of comparison (From Ruohoniemi *et al.*, 1987).

The prototype for the current generation of HF coherent backscatter radars is the Goose Bay HF radar developed by The Johns Hopkins University Applied Physics Laboratory (Greenwald *et al.*, 1985). This radar uses an electronically-steered phased array and operates in the frequency band from 8 – 20 MHz. Measurements are made over a 52° viewing sector centered on 5°E of geographic north and extending from a few hundred kilometers to more than 3000 km in range. Backscatter from F-region ionospheric irregularities is typically observed from 10%–60% of this range interval The radar operates continuously and has provided a wealth of data since its deployment in 1983.

One of the early studies performed with the Goose Bay radar was a comparison of F-region irregularities observed by it with plasma drift velocities observed by the Sondrestrom incoherent scatter radar (Ruohoniemi *et al.*, 1987). This comparison was performed by directing the Sondrestrom radar toward Goose Bay and comparing the observations whenever the scanning Goose Bay radar was pointing

toward Sondrestrom. One of the results of this study is shown in Figure 5. Here the light dotted line represents the Sondrestom radar observations over a 40 minute period and the dark crosses represent the Goose Bay radar observations whenever it is pointing toward Sondrestrom. The sign of the Goose Bay Doppler velocity has been reversed to allow easy comparison of the measurements. It can be seen that the two measurement techniques are in excellent agreement over a broad range of line-of-sight velocities. These observations confirmed an earlier comparison of irregularity and plasma drift by Villain *et al.* (1985) using the SAFARI HF coherent scatter and EISCAT incoherent scatter radars and have been reaffirmed by subsequent comparisons with the Sondrestrom radar and with satellites.

Another study using data from the Goose Bay radar has shown that F-region irregularities may be observed in regions where the ionospheric plasma drift is quite low (Ruohoniemi *et al.*, 1988). While F-region irregularities do not seem to have any velocity threshold, they do seem to be more prevalent when the underlying E-region is dark and when density gradients are present.

In recent years, the Goose Bay radar and an HF radar located at Halley Station, Antarctica and operated by the British Antarctic Survey have been used for the Polar Anglo-American Conjugate Experiment (PACE) (Baker *et al.*, 1989). This investigation is directed toward a broad range of topics in conjugate phenomena with emphasis on plasma convection. Of particular note is the ability of the PACE radars to provide simultaneous images of convection patterns in conjugate hemispheres and to observe changes in these patterns on minute time scales (Greenwald *et al.*, 1990). Figure 6 shows an example of conjugate plasma convection patterns near the cusp for an IMF B_y positive condition, while Figure 7 shows the temporal variations in the northern hemisphere cusp/cleft convection pattern as the IMF B_y changes from a positive to a negative condition. The convection patterns presented in these two figures are derived from single radar observations in each hemisphere. The vector determination procedure is based upon an assumption that the flow is uniform along an L-shell (Ruohoniemi *et al.*, 1989). This assumption is not required with dual-radar common volume measurements. Other studies of convection patterns and convection dynamics based upon data from the PACE HF radars include the observation of convective flow bursts in the vicinity of the cusp (Pinnock *et al.*, 1993) and conjugate observations of the IMF B_y dependence of convection near the Harang Discontinuity (Dudeney *et al.*, 1993). Current work includes the determination of statistical convection patterns for different levels of geomagnetic activity and IMF conditions. Examples of statistical convection patterns for IMF B_z positive and negative are shown in Figure 8.

In order to overcome the limitiations of single radar determinations of drift velocity, a solution similar to the STARE approach was adopted. Following the deployment of the Goose Bay radar, a group of French scientists led by C. Hanuise of LSEET/CNRS redeployed elements of an HF radar that had been used in Scandinavia to Sheffervile, Quebec. In the process, the radar which has become known as SHERPA was upgraded to include most of the features of the Goose Bay system,

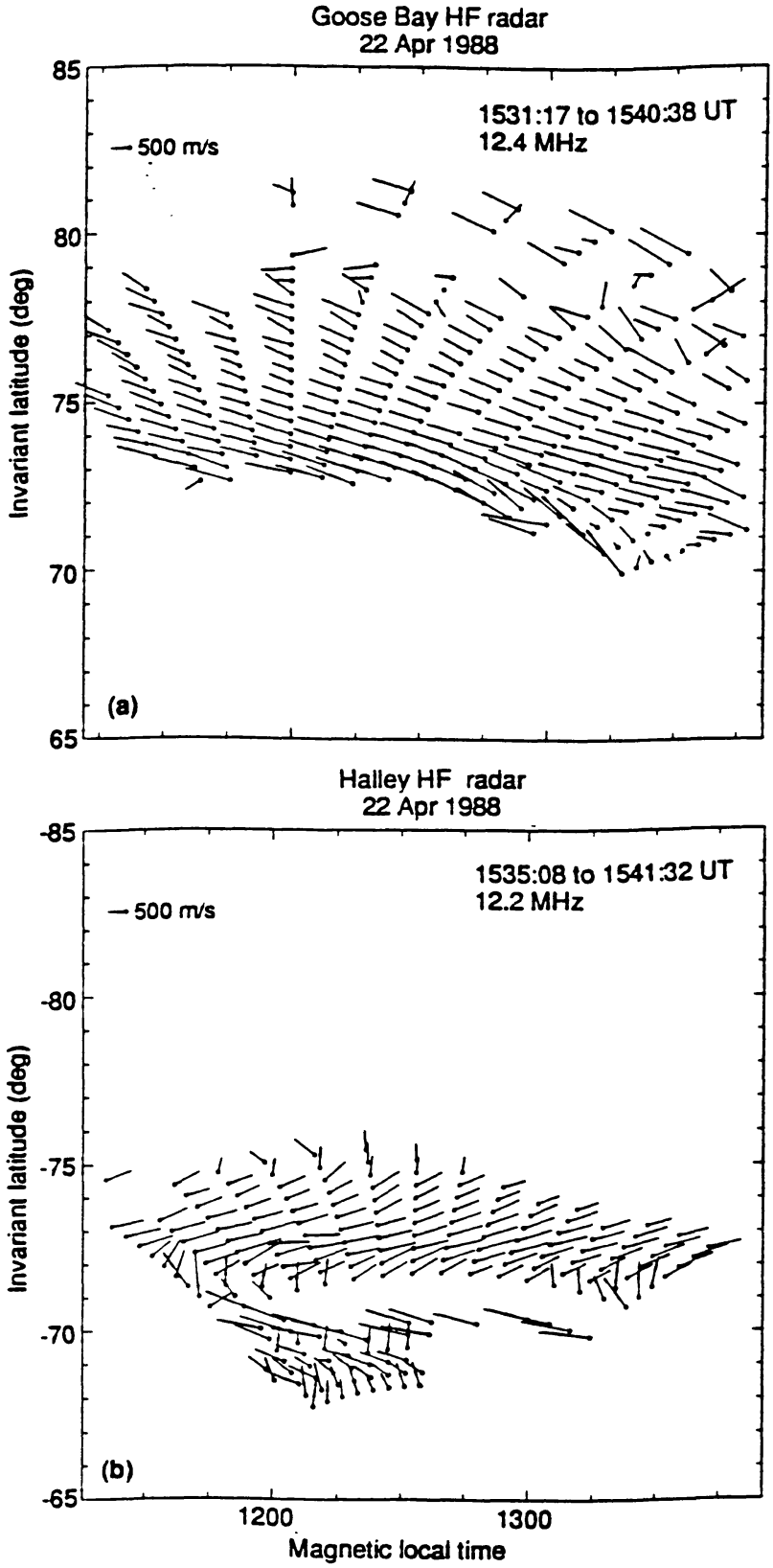

Fig. 6. Simultaneous conjugate observations of F-region plasma drift patterns in the vicinity of the dayside cusp and cleft as observed with the PACE radars at Goose Bay, Labrador and Halley Station, Antarctica. The IMF B_y component was positive and the B_z component was negative at this time (From Greenwald *et al.*, 1990).

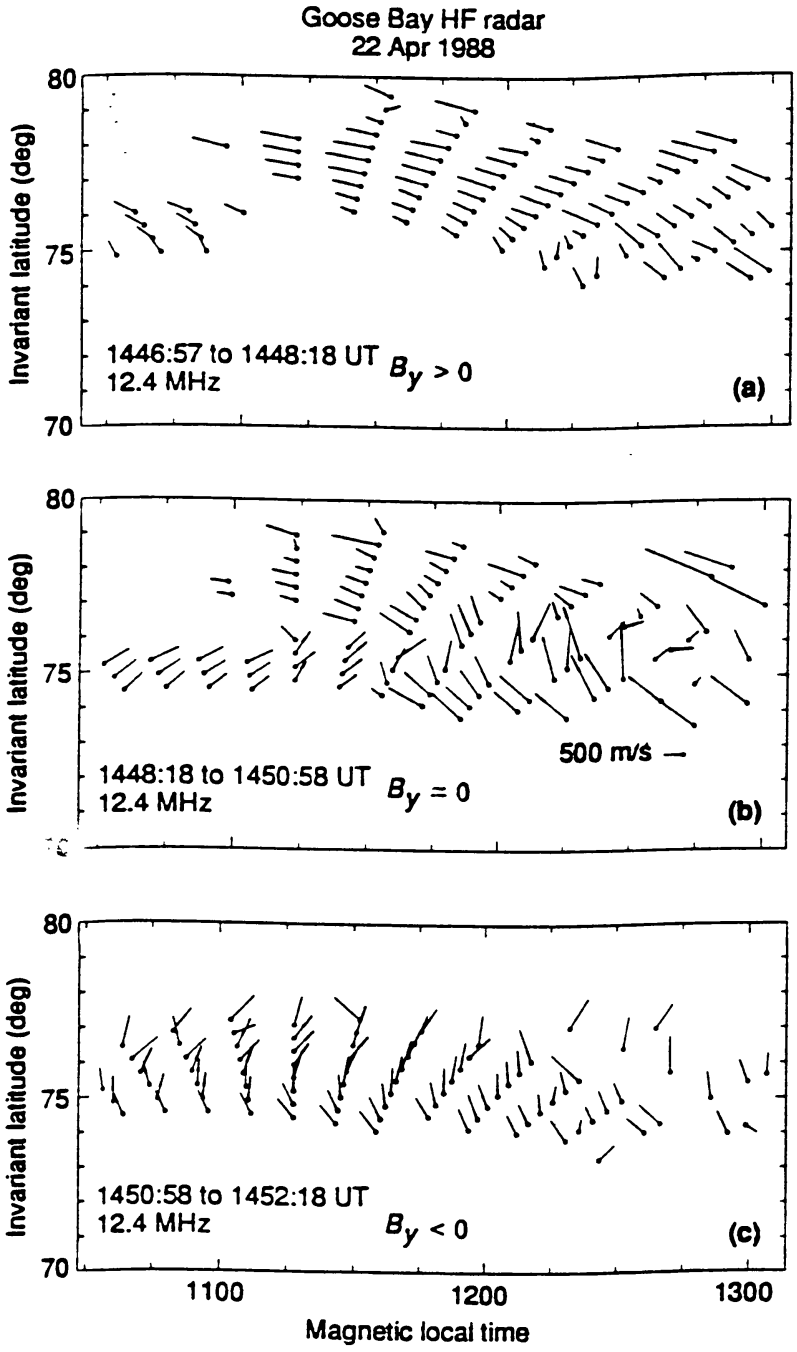

Fig. 7. Goose Bay radar observations of the temporal variation of F-region plasma drift patterns in the vicinity of the cusp and cleft as IMF B_y changes from positive to negative and B_z remains negative (From Greenwald *et al.*, 1990).

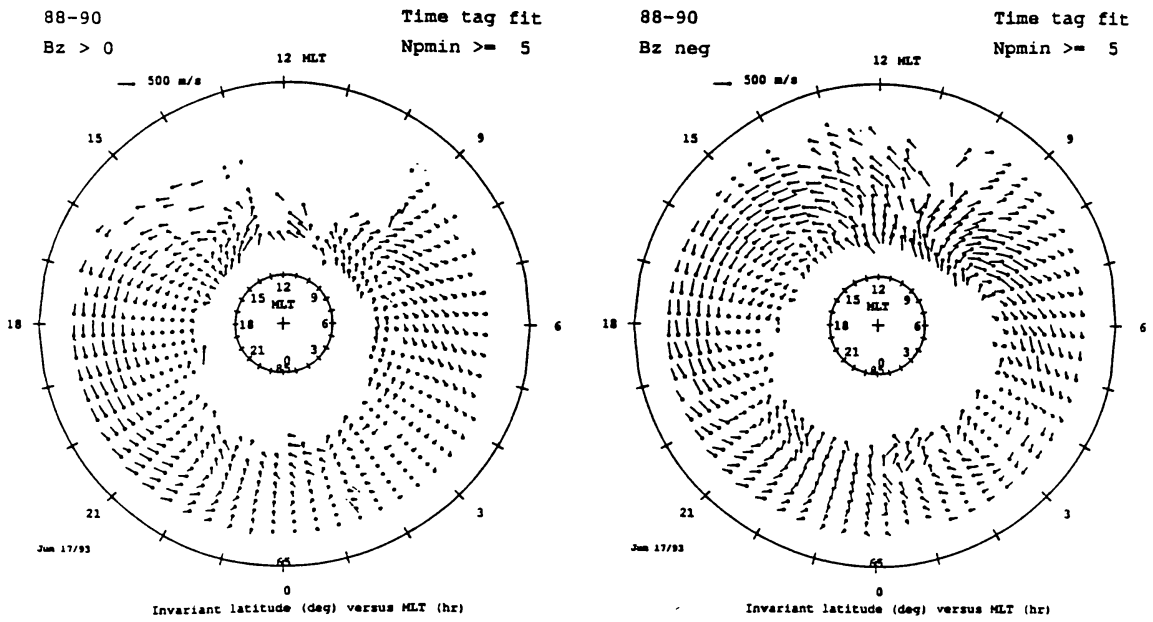

Fig. 8. Statistical patterns of F-region plasma convection for B_z positive and B_z negative as observed with the Goose Bay radar. The patterns are based upon approximately 2 years of data. Each vector is determined from the azimuthal variation of the average Doppler velocity within a fixed local-time invariant-latitude cell as its moves through the field-of-view of the radar.

including the same on-line computer processing and the same electronic scanning capability. Results from the Goose Bay/Scheffervile configuration demonstrated the viability of bi-directional common-volume observations at HF frequencies (Hanuise *et al.*, 1993). Their results also demonstrated the possiblity of separating temporal from spatial variations of convection in the magnetospheric reference frame. By observing the drift velocity profile along a single magnetic median as it rotated through the common field of view of the radars, Hanuise *et al.* (1993) were able to monitor temporal variations of the profile for a 2.5 hour interval with 90 s temporal resolution.

Coordinated observations between the Goose Bay and Schefferville radars are continuing to the present time; however, it is been found that the 500 km spacing between the radars is insufficient for precise vector determination in the higher latitude portion of the radars common viewing area.

2. Scientific Objectives

The principal research objective of the DARN experiment is to provide a global-scale view of the configuration and dynamics of plasma convection in the high-latitude ionosphere. Since plasma convection at high latitudes is largely driven by magnetospheric processes, a global-scale view of convection will provide an

improved understanding of many large scale processes in the magnetosphere-ionosphere-atmosphere system.

In the past, studies of high-latitude convection have largely been statistical. Typically, these studies have used months to years of satellite data (e.g. Heelis, 1984; Heppner and Maynard, 1987), incoherent scatter radar data (e.g. Foster, 1983; Senior *et al.* (1990), de la Beaujardiere *et al.*, 1991) or coherent scatter radar data (Waldock *et al.*, 1985). DARN, particularly the SuperDARN enhancement to DARN, will be the first experiment capable of studying convection over a significant portion of a convection cell on a time scale of just a few minutes. This unique capability will enable us, for the first time, to test various theories of polar cap expansion and contraction under changing IMF conditions and to observe the large-scale response of the nightside convection pattern to substorms.

Much of the energy flow from the magnetosphere is transported into the ionosphere in the form of Joule heating. Large-scale observations provided by DARN will be combined with global-scale measurements of ionospheric conductivity provided by the POLAR imagers to yield a hemispherical determination of the temporal and spatial variability of this important quantity. This large-scale measurement may be supplemented by Joule heating estimates from ground magnetometer arrays and local observations provided by incoherent scatter radar.

Since the high-latitude ionosphere provides an important boundary condition for many of the processes occurring in the magnetosphere, knowledge of the scale and dimension of the electromagnetic properties of these processes within the ionosphere may be of appreciable value in understanding the satellite *in situ* observations. Moreover, the DARN observations will provide a global context for the spatially separated measurements provided by the ISTP/GGS spacecraft. One area in which the global context provided by the DARN observations will be particularly important is that of the large-scale structure of MHD waves. These waves transport electromagnetic energy into the high-latiude ionosphere where it is partially dissipated through Joule heating (Greenwald and Walker, 1980). We plan to use the DARN data along with the ISTP/GGS satellite data to measure the energy influx from these waves on a larger spatial scale than has heretofore been possible.

DARN measurements will also be used to study the dynamics of nightside convection during substorms. This is another area in which a global view will provide new insight into one of the most important processes coupling the magnetosphere and ionosphere. It is also an area where the DARN measurements will help to provide a global context to the GEOTAIL and POLAR observations.

HF radars have been found to be excellent sensors of atmospheric gravity waves excited in and propagating through the high-latitude ionosphere. These waves are of importance since they can transfer appreciable amounts of energy between the high-latitude and lower-latitude atmosphere. They can also transfer energy to different altitudes within the atmosphere. Gravity waves are sensed with HF radars because they produce a corrugated structure in the electron-densitiy profiles on

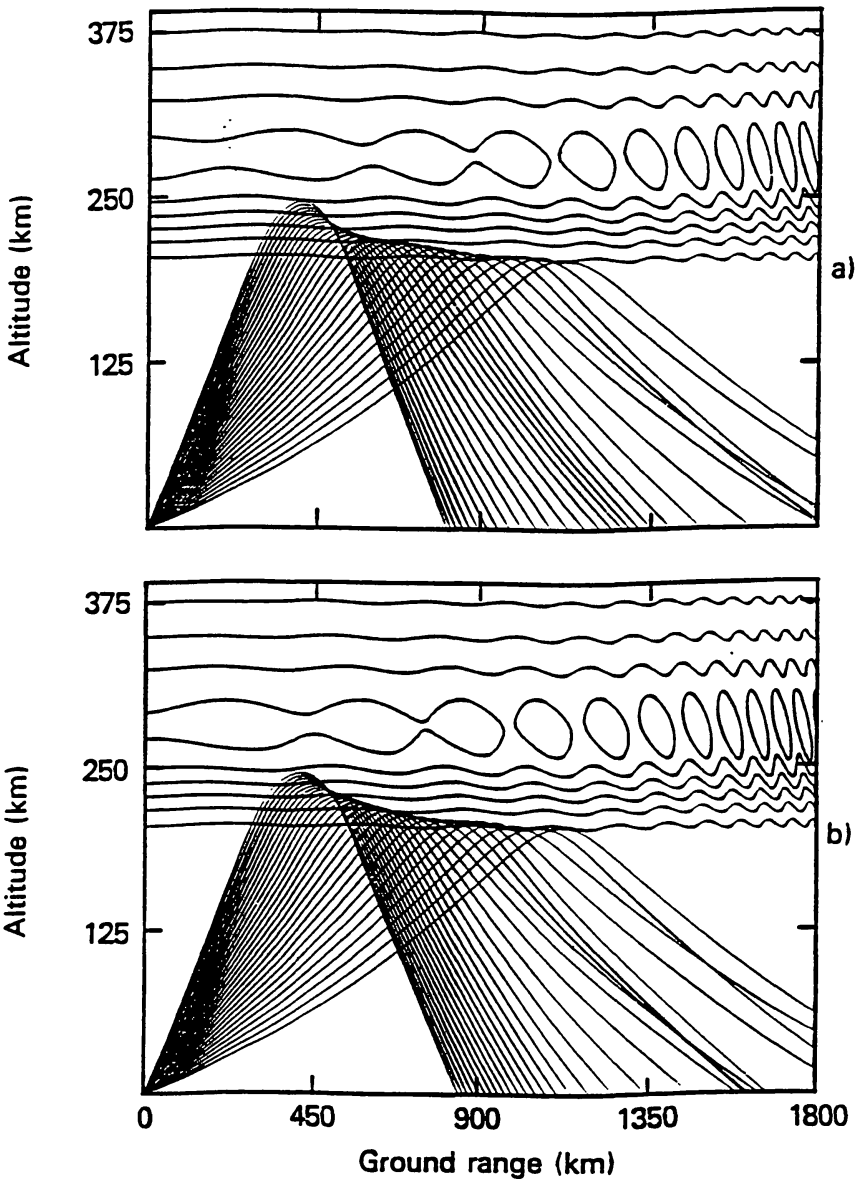

Fig. 9. Schematic view of the manner in which a corrugated ionosphere produced by a atmospheric gravity wave can focus and defocus radar signals. In this example, both the gravity wave and the ground range of focused radar signals are moving toward the radar site. The two examples are separated by 15 minutes (From Samson *et al.*, 1990).

the bottomside of the ionosphere. The corrugated structures produce alternating regions of focusing and defocusing of the radar signals reflected off the bottom of the ionosphere as indicated in Figure 9. As the gravity waves move, the location of the ground backscatter return may be tracked and the source location of the gravity wave may be determined (Samson *et al.*, 1990). Recent studies using the Goose Bay radar have confirmed that the source of many high-latitude gravity waves packets are surges in the high-latitude current systems (Bristow *et al.*, 1994).

Finally, the radars' inherent ability to detect ionospheric structure will provide a global view of the plasma instability processes that occur in the high-latitude ionosphere.

The following table summarizes the research topics that will be investigated with the DARN data. It also indicates some of the special attributes of DARN that will allow these studies to be completed and it indicates other important instrumentation for completing the research.

3. Instrument Description

3.1. Evolution of DARN and SuperDARN

The research accomplishments with the STARE radars during the late 1970s led to the development of additonal VHF radar pairs. These included the SABRE radar system operated from Wick, Scotland and Upsaala, Sweden (Nielsen *et al.*, 1983) and the BARS radar system operated from Red Lake, Ontario and Nipawin, Saskatchewan (McNamara *et al.*, 1983). All of these radars and three additional planned sites were part of the Dual Auroral Radar Network (DARN) proposal that was submitted to NASA in response to the Announcement of Opportunity for the Origins of Plasmas in the Earth's Neighborhood (OPEN) mission. Each viewing area was to extend over about 1 hour in magnetic local time and 4° in latitude. Figure 10 shows the DARN network as it was depicted in the original proposal. At that time, the STARE radars (Region 2) were in operation, while the SABRE radars (Region 3) were under construction, the BARS radars (Region 8) were being planned and the remaining DARN sites (5, 7, and 9) were being considered. Note that Region 5 represents a conjugate mapping of two radars that were being considered for operation in Antarctica.

During the early 1980s, as some of the shortcomings of the E-region coherent scatter technique were becoming more apparent, French and Swedish scientists initiated a series of HF investigations of the high-latitude F-region in northern Scandinavia (Hanuise *et al.*, 1981). These studies were followed by preliminary studies of F-region coherent backscatter from Alaska (Greenwald *et al.*, 1983) and eventually by the development of the previously noted Goose Bay HF radar (Greenwald *et al.*, 1985). Each of these radars involved certain technical and/or operational improvements over its predecessors with the Goose Bay radar having

TABLE I
Scientific Goals of DARN/SuperDARN

Topic	DARN requirements	Additional instrumentation and data of particular usefulness
Structure of Global Convection	• extended coverage in MLT and magnetic latitude. • moderate spatial (~100 km) and temporal (~10 min) resolution	• Collaboration with modelers • Incoherent scatter radars • Ground magnetometer chains • Solar wind parameters
Dynamical Studies of Global Convection	• Extended, continuous coverage in MLT and magnetic latitude • Good spatial (~50 km) and temporal (~ 2 min) resolution • Multi-directional observations of common volume to determine instantaneous 2-D velocity vectors	• Plasma diagnostics from ISTP satellites • Incoherent scatter radars • Magnetometer and optical imager data • Conjugate radar observations • IMF and solar wind parameters
MHD Wave Studies	• Extended, continuous coverage in MLT and magnetic latitude • Good spatial (~50 km) and temporal (~ 2 min) resolution • Multi-directional observations of common volume to determine instantaneous 2-D velocity vectors	• Ground magnetometer chains • ISTP optical imager data • IMF and solar wind parameters • Plasma diagnostics from ISTP satellites
Substorm Studies	• Extended coverage in MLT and magnetic latitude • Good spatial (~50 km) and high (~1 min) temporal resolution • Multi-directional observations of common volumes to determine instantaneous 2-D velocity vectors	• Magnetometer and optical imager data • Conjugate observations from radars, magnetometers, and imagers • IMF and solar wind parameters
Gravity Wave Studies	• Large area coverage • Continuous operation • Good spatial (~50 km) and moderate temporal (~ 10 min) resolution	• Optical and/or incoherent scatter radar data to provide conductivities and Joule heating rates • Density profiles from ionospheric sounders

TABLE I

(continued)

Topic	DARN requirements	Additional instrumentation and data of particular usefulness
High Latitude Plasma Structure Studies	• Large field-of-view, including the polar cap regions. • Continuous monitoring of the source region(s)	• Polar cap all-sky cameras and photometers • Ionospheric sounders and/or incoherent scatter radars.
Ionospheric Irregularities	• Multi-frequency observations of common volumes • High temporal (~ 1 min) and high spatial (~ 30 km) resolution	• Plasma diagnostics from ISTP satellites and incoherent scatter radars • Field-aligned current measurements from satellites • Scintillation measurements for km-scale irregularity structures • VHF radar measurements for use in conjunction with multi-frequency HF observations

an electronic scanning capability and the ability to operate continuously. Next, the French SHERPA radar was developed at Schefferville.. Finally, a third HF radar was developed jointly by the British Antarctic Survey and JHU/APL, and deployed at Halley Station, Antarctic as part of the Polar Anglo-American Conjugate Experiment (PACE).

Although the current constellation of HF radars have yielded a broad range of interesting results on the structure and dynamics of high-latitude plasma convection, the analyses have suffered some limitations. The primary limitation of most of the research reported to date is that only one Doppler component is available from each spatial volume probed with the radar. In order to obtain vector velocity determinations from this type of radar data, Doppler measurements must be made of different spatial volumes and these must be combined using one or more physical assumptions. Ruohoniemi *et al.* (1989) have described the procedures and assumptions that are currently used in deriving velocity vectors from HF coherent-scatter radar data. They have also developed techniques for merging Goose Bay data with Sondrestrom data for direct vector determination and they have found that the two approaches generally yield similar results. Nevertheless, Freeman *et al.* (1991) have shown that failure of one or more of the assumptions used in the single radar analysis could lead to gross errors in the velocity estimate. Under worst conditions, the flow directions could be in error by as much as 180°! Freeman *et al.* (1991) have also concluded that it is impossible to know when the results are correct and when they are in error.

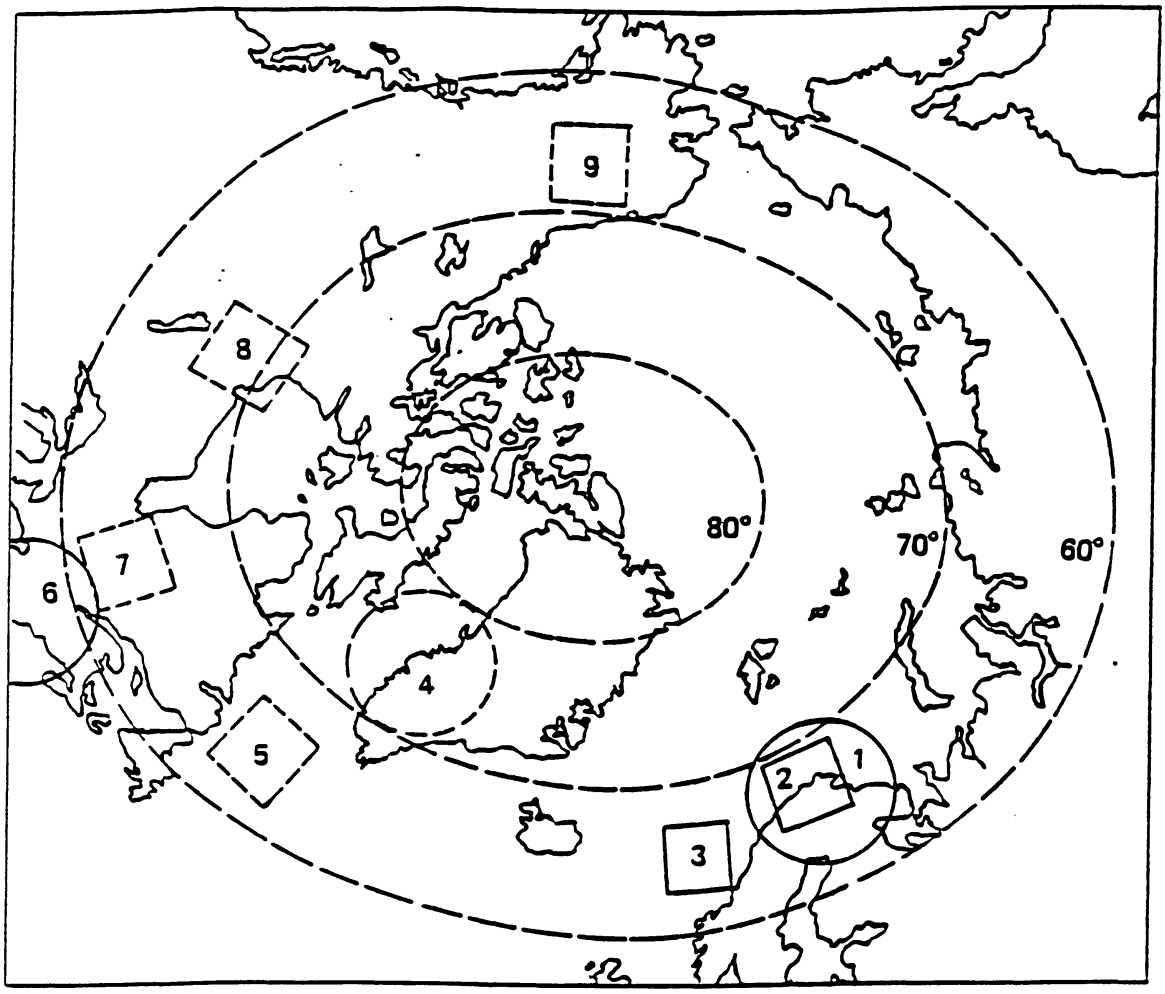

Fig. 10. Plan view of northern polar region from original DARN proposal showing fields-of-view of existing (solid) and proposed (dashed) coherent scatter (squares) and incoherent scatter (1000 km circles) radar systems. Region 5 is a conjugate mapping of two antarctic radars.

By the end of 1989, it became apparent that bi-directional common-volume observations with radar separations significantly greater than 500 km were the best approach to advancing the study of high-latitude convection with HF radars. On considering alternative sites for a radar to be operated in coordination with the Goose Bay radar, several interesting characteristics of paired HF radar deployment became apparent:

> Firstly, the common field-of-view of two appropriately sited HF radars is extremely large. In area, it is roughly seven times greater than that of STARE. Typically the common field-of-view will cover 15°–20° of invariant latitude and 3 hours of magnetic local time. This large common area results from the extended range coverage of an HF radar, ~3000 km, and the 52° azimuthal

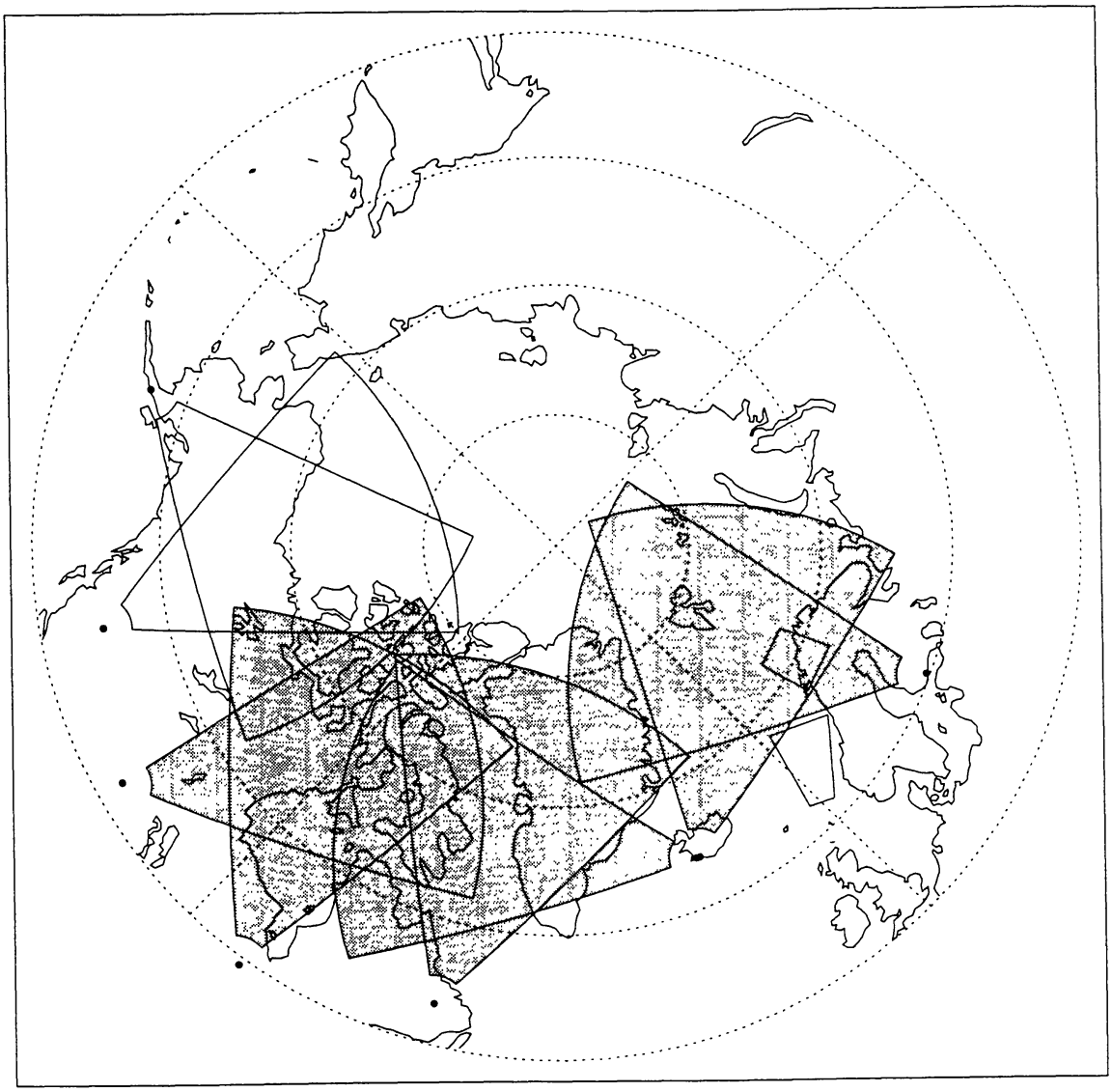

Fig. 11. Fields-of-view of funded (shaded) and planned (unshaded) northern-hemisphere Super-DARN HF radars as well as the STARE radar in northern Scandinavia and the remaining SABRE radar in Wick, Scotland.

coverage. These values are to be compared with 1200 km maximum range and 26° azimuthal coverage for STARE.

Secondly, the fields-of-view of several pairs of HF radars extend the spatial coverage of the high-latitude auroral zone and polar cap boundary over many hours of magnetic local time. If ionospheric irregularities were to fill this common viewing area, it would be possible to monitor the dynamics of plasma convection over a significant part of a convection cell. Moreover,

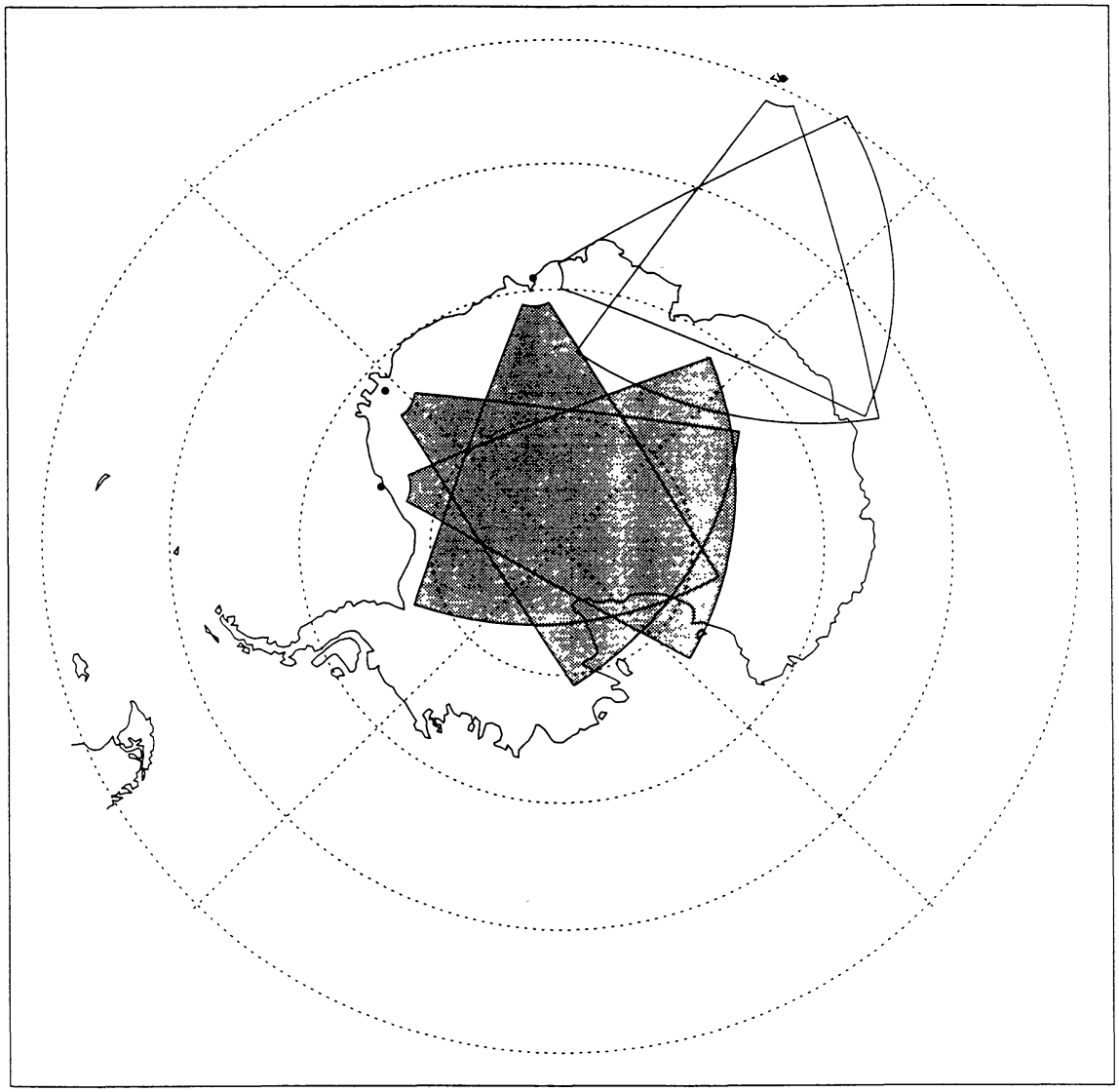

Fig. 12. Fields of view of funded (shaded) and planned (unshaded) southern-hemisphere SuperDARN HF radars.

it is possible to monitor large-scale processes that affect convection over the same local time extent.

Thirdly, the goals of bidirectional radar coverage and extended local time measurement can be achieved with a relatively modest number of radars. Four pairs of HF radars can provide spatial coverage over 260° of geographic longitude. The common viewing area would include Alaska, northern Canada, Greenland, and northern Scandinavia, including Svalbard.

Finally, in the southern hemisphere extended spatial coverage is more difficult to achieve due to the sparsity of land masses and/or station sites.

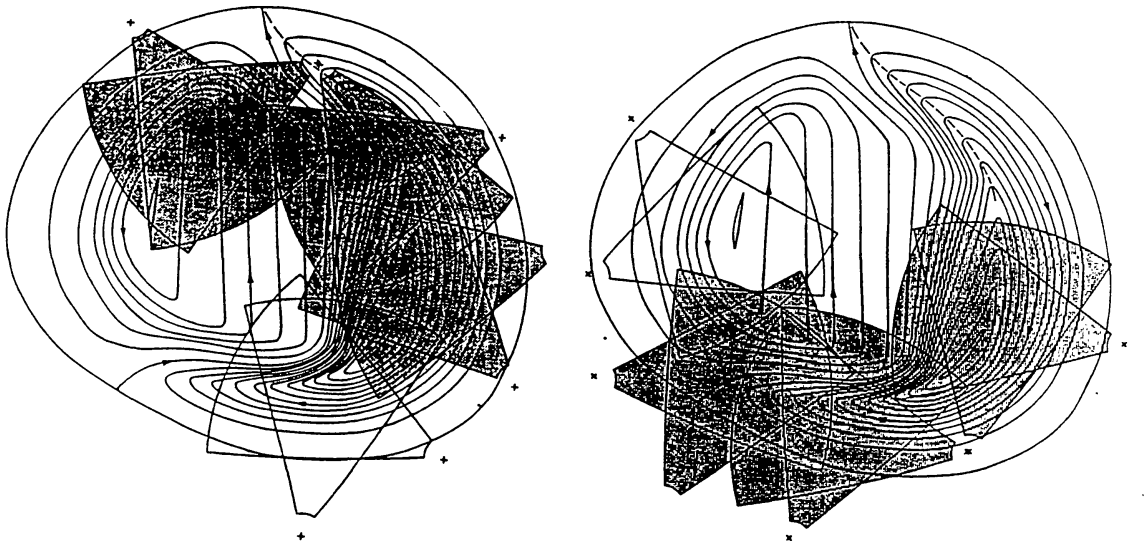

Fig. 13. Heppner-Maynard Model DE convection pattern with superimposed coverage provided by northern-hemisphere SuperDARN HF radars. Left panel: Coverage of dayside convection. Right panel: Coverage of evening and nightside convection.

Nevertheless, it is still possible to select several Antarctic and sub-Antarctic sites that can provide conjugate viewing of part of the northern hemisphere viewing area.

With these issues in mind, the DARN Investigation Team, along with a representative from the Canadian Network for Space Research, at a 1990 meeting in Lindau, Germany considered how their respective countries might contribute to a global-scale HF radar network that would significantly expand the coverage and capability of the DARN investigation. The new network was given the acronym, SuperDARN, to signify that it was derived from the DARN concept, but that it was significantly larger in scope. At a follow-up meeting at JHU/APL later that year the responsiblites for the development and funding of the various radars were distributed to the participants. It is very gratifying to note that all of the resulting proposals for funding have eventually been supported.

3.2. Elements of DARN/SuperDARN

The initial conception for SuperDARN was to have 8 northern hemisphere radars sited at 5 locations and 2 southern hemisphere radars sited at 2 locations. This conception has evolved with time, most notably in the decision to site the radars at separate locations, if possible, and in the number of southern hemisphere radars. At the current time, the sites of the funded radars and their anticipated start of operations are given as follows:

TABLE II

Northern Hemisphere			
Location	*Geographic Coordinates*		*Initial Operation*
Saskatoon, Sas, Can.	52.2° N	−106.5° E	Operational
Kapuskasing, Ont, Can.	49.4° N	−82.3° E	Operational
Goose Bay, Lab, Can.	53.3° N	−60.5° E	Operational
Stokkseyri, Iceland	63.9° N	−21.0° E	June, 1994
Iceland East	TBD		Summer, 1995
Finland	TBD		Autumn, 1994

Southern Hemisphere			
Location	*Geographic Coordinates*		*Initial Operation*
Halley Station, Antarctica.	75.5° S	−26.6° E	Operational
SANAE, Antarctica	72.0° S	−3.0°E	January, 1996
Syowa, Antarctica	69.0° S	39.6° E	January, 1995

There are also several locations being considered for unfunded SuperDARN radars. In the northern hemisphere, these sites are in British Columbia, Canada and King Salmon, Alaska, while in the southern hemisphere, a second radar would be located at Syowa and a French radar would be located at Kerguelen Island. Figure 11 shows the combined fields-of-view of the funded and planned elements of SuperDARN in the northern hemisphere as well as the continuing European VHF radars that are part of DARN. The SuperDARN viewing areas are defined by the full azimuthal scan of each radar and the range interval over which the backscattered returns are sampled (typically 180–3285 km). A similar procedure is used for the SABRE radar, whereas the STARE radar only indicates the common viewing area. The Canadian BARS radars is not indicated in this figure since a description of BARS is included as part of the CANOPUS experiment. Figure 12 shows the fields-of-view of the existing and planned SuperDARN radars in the southern hemisphere.

The ability of SuperDARN to image large portions of the high-latitude convection pattern is amply illustrated in Figure 13. Here, the fields-of-view of the northern-hemisphere SuperDARN station configuration have been projected onto the dayside (left panel) and afternoon-evening (right panel) portions on the Heppner-Maynard DE pattern. In the first case, it can be seen that the radars' fields-of-view extend over the full dayside portion of both the dawn and dusk convection cells and that they provide excellent coverage of convection associated with the

cusp and magnetospheric boundary layer. In the second case, it can be seen that SuperDARN has the potential of imaging a full convection cell. These examples indicate that SuperDARN should provide views of magnetospheric and ionospheric electrodynamics that have heretofore only been available through less direct techniques, e.g. Assimilative Mapping of Ionospheric Electrodynamics (AMIE) (Richmond and Kamide, 1988).

The Principal Investigators (PIs) for the funded elements of SuperDARN and their respective funding agencies are as follows:

Saskatoon
Prof. George Sofko
Institute of Space and Atmospheric Studies
University of Saskatchewan
Saskatoon, Saskatchewan S7N 0W0
Canada
E-Mail: CANSAS::Sofko
Funded by the Natural Sciences and Engineering Research Council (NSERC) of Canada

Kapuskasing and Goose Bay
Dr. Raymond A. Greenwald
The Johns Hopkins University/Applied Physics Laboratory
Johns Hopkins Road
Laurel, MD 20723
USA
E-Mail: APLSP::Greenwald or ray_greenwald@spacemail.jhuapl.edu

Kapuskasing is funded primarily by the National Aeronautics and Space Agency (NASA) with additional support from the Institut National Science de l'Univers (INSU); Goose Bay is funded by the National Science Foundation (NSF)

Stokkseyri, Iceland
Dr. Jean-Paul Villain
3A Avenue de Recherche Scientifique
45071 Orleans Cedex 2
France
E-Mail: jvillain@cnrs-orleans.fr

Funded primarily by INSU with additional support from DRET, IFRTP, and NSF

CUTLASS:(Iceland East and Finland)
Prof. Tudor B. Jones

Department of Physics and Astronomy
University of Leicester
University Road
Leicester, LE17RH. U.K.

Funded by the Science and Engineering Research Council (SERC) with additional support from Finland and Sweden. SERC also funds the operation of the SABRE VHF radar located at Wick, Scotland.

Halley
Dr. John Dudeney
British Antarctic Survey
High Cross, Madingley Road
Cambridge, CB3 0ET. UK.
E-Mail: Dudeney@pcmail.nerc-bas.ac.uk

Funded by the Natural Environment Research Council (NERC) and NSF

SANAE
Prof. A. David M. Walker
University of Natal
Durban, Republic of South Africa
E-Mail: Walker@lola.ph.und.ac.za

Funded by the Department of Environmental Affairs, Republic of South Africa with additional support from NERC and NSF

Syowa
Prof. Natsuo Sato
Japanese Institute of Polar Research
Tokyo, Japan

Funded by the Japanese Ministry of Education

The potential contribution of the VHF radars to the DARN database is a topic of some uncertainty at the present time. The remaining SABRE radar is located at Wick, Scotland and operated by the University of Leicester. Due to funding contraints, this radar will be decommissioned as the CUTLASS radars become operational.

The STARE radars are also faced with an uncertain future. An extensive upgrade has required several years of effort and has not as yet been successfully completed. Moreover, radio interference problems have recently arisen with the STARE radar in Malvik, Norway. These problems may require that that radar be relocated to a

more isolated site. Currently, there is no Key Parameter software for the STARE system.

The Principal Investigators and funding support for the upgraded STARE radars are:

STARE

Funded by the Max Planck Society and the Finnish Meterological Institute

Dr. Erling Nielsen
Max Planck Institut fuer Aeronomie
3411 Katlenburg-Lindau, Germany

Dr. Risto Pellinen
Finnish Meteorlogical Institute
Helsinki, Finland

3.3. Detailed Description of the SuperDARN Radars

The HF radars comprising the SuperDARN component of DARN are based upon the design of the Goose Bay HF radar as described in Greenwald *et al.* (1985). These radars utilize ionospheric refraction to achieve orthogonality with the magnetic field in the high-latitude F-region. Since the amount of refraction is dependent upon the ionospheric electron density which varies diurnally, annually, and with geomagnetic activity, an HF radar must be capable of operating over an extended frequency range. All of the SuperDARN radars cover the frequency range from 8 to 20 MHz, which enables them to achieve similar operational conditions over a factor of more than six in peak electron density. The radars are also frequency agile, allowing observations at two or more different frequencies to be interwoven.

The main antenna array used with the SuperDARN radars consists of 16 log-periodic antennas. Signals from or to these antennas are phased with electronically-controlled time-delay phasing elements that allow the beam to be steered into 16 directions covering a nominal 52° azimuth sector. The azimuthal resolution of the measurements is dependent on radar operating frequency and ranges from 2.5° at 20 MHz to 6° at 8 MHz. Since most of the observations are made in the frequency range from 12–14 MHz, the nomimal azimuthal resolution of the radar is 4°. At a range of 1500 km, this corresponds to a tranverse spatial dimension of ~100 km.

In addition to the main antenna array, a secondary, parallel array of 4 antennas is used to determine the vertical angle of arrival of the backscattered signal. The second array also uses a phasing matrix and is located 100 m in front of or behind the primary array. It functions as an interferometer to determine the relative phases of the backscattered signals arriving at the two arrays. This phase information is converted to an elevation angle, which is used to determine the propagation modes of the returning signals as a function of range, as well as the approximate altitude of the scatterers. The secondary array is only used for reception. It does not need to be of the same length as the main array since only the correlated portion of the signals incident on the two arrays is of importance for angle-of-arrival determinations. A view of the SuperDARN antenna arrays at Kapuskasing, Ontario is shown in Figure 14.

Fig. 14. View of antenna arrays of the SuperDARN HF radar located at Kapuskasing, Ontario.

The range resolution of the SuperDARN measurements is determined by the transmitted pulse length which is typically 200–300 ms or equivalently 30–45 km.

SuperDARN electronic steering occurs on microsecond time scales, allowing the radar to be scanned rapidly through a number of beams or to dwell for an extended period on a single beam. While a wide range of scan sequences are possible, the Goose Bay and Halley radars typically scan in a sequential fashion with a dwell of 6 s in each beam direction and a full-scan time of 96 s. As the new SuperDARN radar pairs come on line, they will need to operate in a synchronous manner. The basic northern-hemisphere scan pattern for a pair of radars will be to scan the more westward radar in a clockwise direction and the more eastward radar in a counterclockwise direction. The sense of the scans will be reversed for the southern hemisphere radars. The scans will be initiated every 2 min of the hour and the dwells in each position will last for 7 s. With synchronization of the viewing direction of the radars, the instantaneous common viewing area will track from north to south during each scan. Other positions within the common field-

of-view of the radars will be monitored at different times and therefore be subject to potential error due to short-term temporal variability in ionospheric convection. An alternative approach, not yet under development, will be to change the beam direction rapidly and integrate the observations from all viewing directions over a 1–2 minute period. This will ensure that concurrent observations are made over the full, common field-of-view; however it will also increase the temporal averaging of the observations.

These scan modes are two of many possibilities. Significantly higher temporal resolution can be achieved over a limited portion of the radar scan and high and low temporal resolution observations over limited and full scans can be made simultaneously.

The SuperDARN radars use broadband (8–20 MHz) solid state transmitters located in weatherproof containers at the base of each antenna of the main array. Each transmitter has an peak output power ranging from 500–800W across the frequency band and a duty cycle of up to 6%. Due to the modest transmitted powers and low duty cycle, less than 2kW of power are required to operate each radar. Consequently, the SuperDARN radars are operated continuously with little regard to the power costs. On the other hand, the peak effective radiated power (ERP) of each radar as computed from the peak pulse power and the antenna gain is in excess of 3MW.

The radars are controlled by a fast micro-computer system (a 66 MHz Intel 80486) running a real-time operating system (QNX®, QNX Ltd., Toronto, Canada). This system is extremely flexible and can be used to modify virtually all of the operating parameters of a radar. Changes in operation can be performed directly by an operator, under program control in response to a specific schedule, or under program control in response to changing ionospheric conditions as observed by the radar. A radar may also be controlled remotely using a standard telephone modem, enabling very complex experiments to be conducted without an operator actually being located at the radar site. Some real-time data (limited by the 9600 baud rate of the modem) can be selected and transferred to the remote experimenter for monitoring purposes.

The SuperDARN radars use a number of different multipulse transmission sequences consisting of 5 to 7 pulses transmitted over a 100 ms time period. The backscatter returns from these pulses are sampled and processed to produce multi-lag autocorrelation functions (ACFs) as a function of range. A multipulse pattern is a staggered, non-redundant lag sequence from which the backscatter ACFs can be uniquely determined as a function of range.

The ACFs are fitted to determine the backscattered power, the mean Doppler velocity, and the width of the Doppler power spectrum for each range where there are significant returns. These estimates are produced in real-time and stored along with the complete autocorrelations functions on an optical disk.

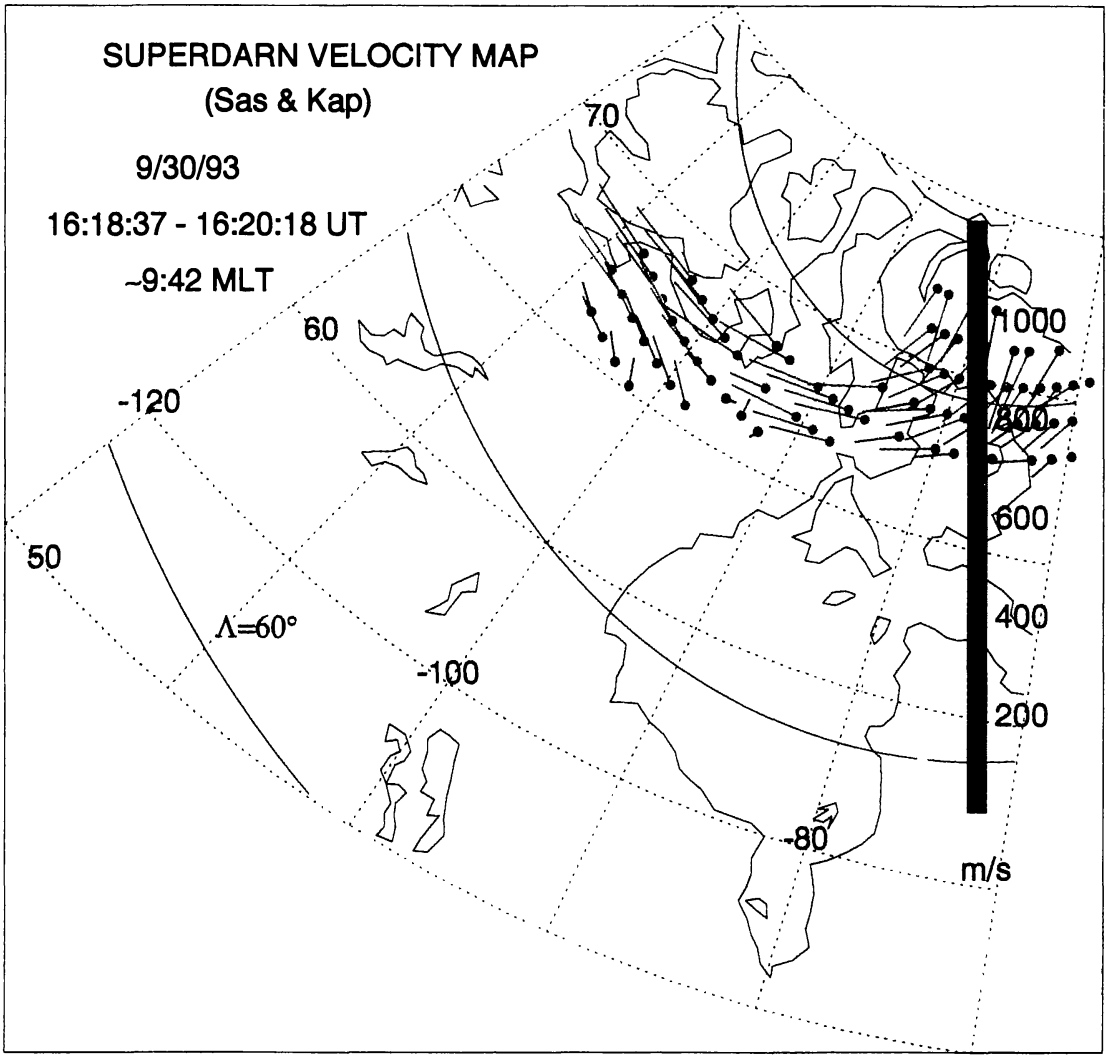

Fig. 15. Convection map of the dayside high-latitude ionosphere obtained with the Kapuskasing and Saskatoon SuperDARN radars. The dots represent the location of each vector determination. The direction of the line represents the flow direction and the length and color of the line the flow magnitude. In this example the flow is sunward out of the polar cap at ~11 MLT and rotates westward as it moves to lower latitude.

3.4. Examples of SuperDARN Data

The new Saskatoon and Kapuskasing radars have been operating intermittently since July and nearly continuously since October 1993. From this data set a wealth of interesting observations have been obtained and are now being subjected to detailed analysis. Examples of these observations are presented in Figures 15–17. The vectors shown in these figures are derived using procedures that have been developed for common-volume observations between Goose Bay and Schefferville and between Goose Bay and the Sondrestrom incoherent scatter radar. A more

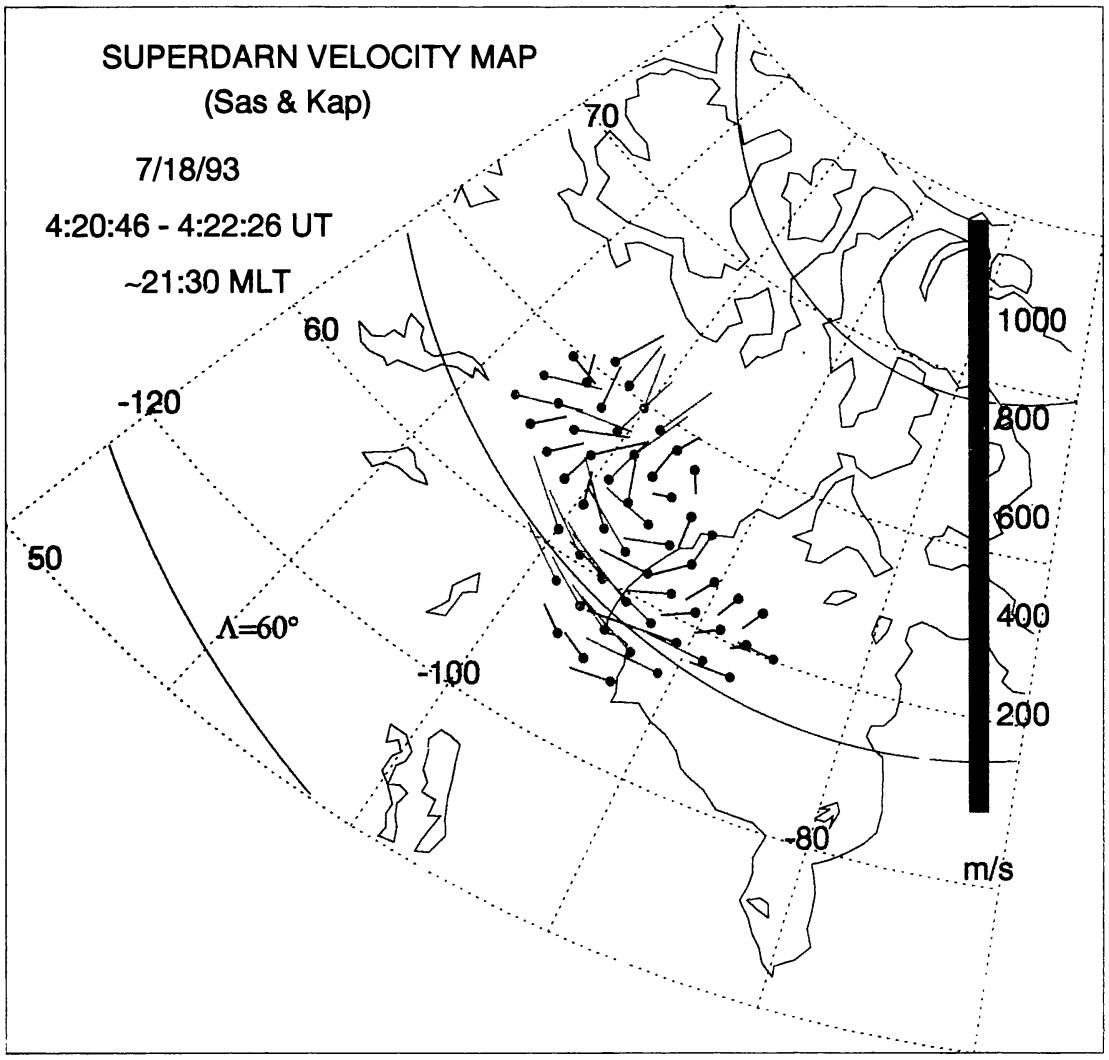

Fig. 16. Convection map of a portion of the dusk convection cell near 18 MLT.

advance technique is currently under development and will be reported on in the near future.

The first example, Figure 15, is of a segment of a reverse convection cell in the high-latitude dayside ionosphere observed presumably under northward IMF conditions. The dot associated with each of the vectors is the location of the measurement. The direction of the line represents the flow direction and the length of the line and color are used to indicate the flow magnitude. Sunward-directed flow is observed exiting from the polar cap at approximately 80° invariant latitude and 11 MLT. This flow rotates westward and antisunward as it moves to lower latitudes and earlier local times. The overall pattern is similar to the sunlit northward-IMF polar-cap convection patterns described by Burke *et al.* (1979). This is the first time that such clear examples of sunward polar-cap flow have been derived from HF radar data.

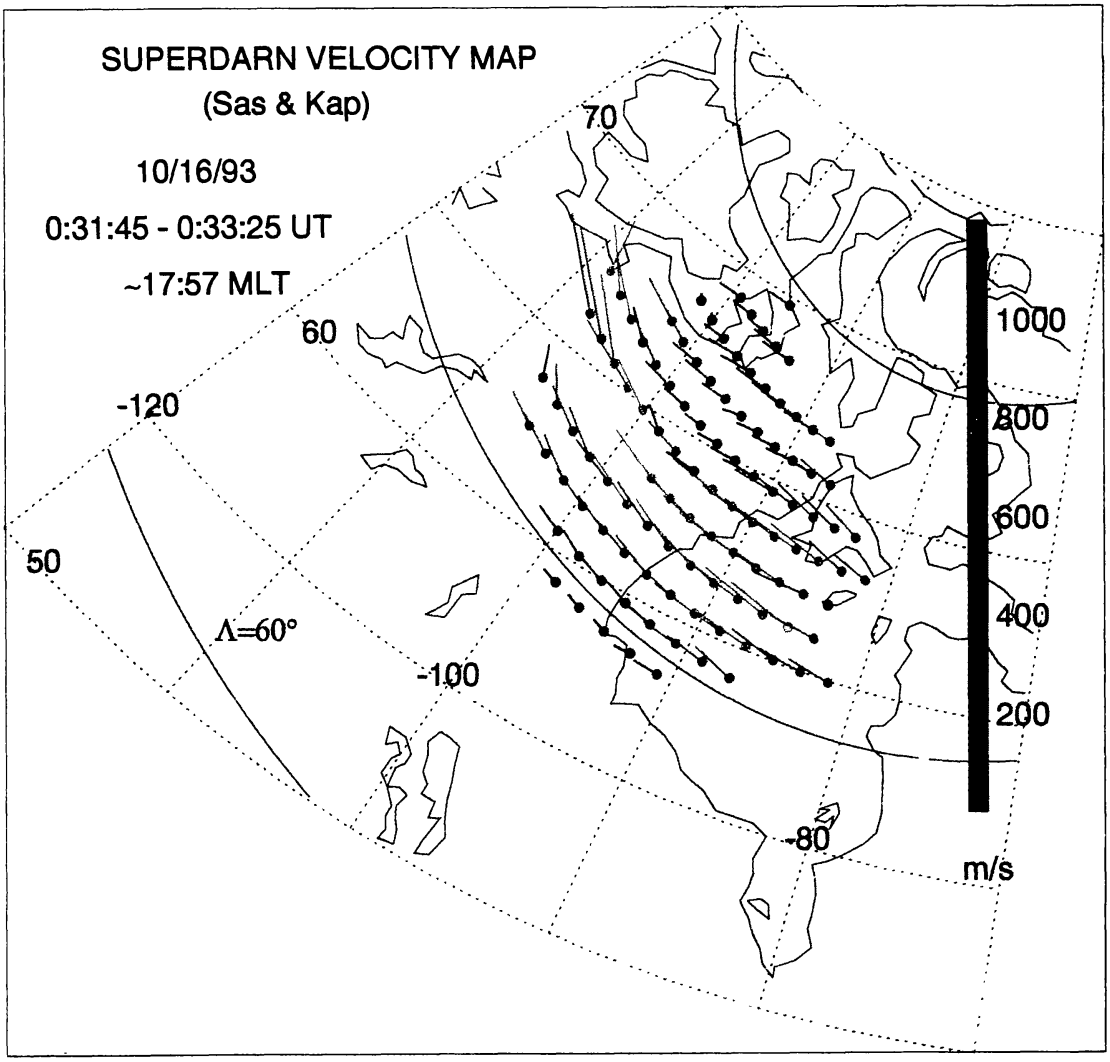

Fig. 17. Convection map of a flow vortex associated with a bipolar magnetic transient observed near 2130 MLT. The vortex moved westward and may have been associated with a westward traveling surge. Optical data were not available due to the season.

Figure 16 is an example of dusk cell convection near the dusk meridian. In this example, backscatter is observed from an irregularity zone that is approximately 10° in latitudinal extent and the associated convection maximizes near 73° invariant latitude. The total dusk-cell potential drop observed at this time is approximately 20 kV.

Finally, Figure 17 depicts a convection vortex that was observed briefly in association with a bipolar magnetic transient near 2130 MLT on 18 July 1993. The vorticity is consistent with a region of upward field-aligned current and the overall pattern is similar to the STARE observations of a westward traveling surge that were shown in Figure 2. This pattern appeared as a westward moving transient that

evolved into a region of high speed, ~1500 m/s, laminar flow which lasted for ~15 minutes.

These examples are characteristic of the observations that will be obtained with the SuperDARN radars. Typically, a radar pair observes backscatter within the region of common volume observations over several hours of local time and 4°–10° in latitude. Backscatter can also be observed equatorward of the common volume region, but vector determinations then rely on the analysis techniques reported by Ruohoniemi *et al.* (1989) and care must be exercised to identify E-region backscatter.

3.5. Operations

The SuperDarn radars will operate continuously providing a global-scale diagnostic of the electrodynamic state of the high-latitude ionosphere. Data from the northern hemisphere radars will be collected at JHU/APL where it will be put onto high-capacity exabyte tapes and distributed to the PIs in the participating countries for subsequent redistribution to interested scientists. Selected portions of these tapes will also be made available to national data centers to support the activities of national and international research programs. Details for the collection of the southern hemisphere data onto exabyte tape still need to be worked out. The primary difficulty is that the full data suite from the southern hemisphere radars can only be assembled after the optical disks are retrieved from Antarctica, approximately one year after the data are acquired.

Key Parameter data will be produced at both the northern and southern hemisphere radar sites and submitted to the ISTP/GGS Central Data Handling facility (CDHF) within 48 hours of acquisition. The Key Parameters are continuous estimates of the latitudinal profile of the ionospheric plasma convection velocity (equivalent to electric field profiles) along the central meridian of the radar. The profiles will typically extend over 4°–10° within the range from 63° to 85° geomagnetic and have a latitudinal resolution of ~0.5° and a temporal resolution of 90–96s. These profile estimates are determined using the techniques described by Ruohoniemi *et al.* (1989). They are collected for 24 hour intervals and transmitted to JHU/APL on a nightly basis. After verification at JHU/APL, they are transmitted to the CDHF for inclusion in the Key Parameter File. Every effort will be made to submit this data to the CDHF in a timely fashion.

As the SuperDARN radar pairs become operational, Doppler data from specific ranges on each beam will also be included in the Key Parameter data sent to JHU/APL. At JHU/APL, these data will be combined with similar Doppler data from the companion radar to determine merged vector velocity profiles. Vectors obtained in this manner will have somewhat poorer latitudinal resolution than the single radar determinations. However, they are more rigorously determined and will replace the single radar velocity estimates when they are available. The revised Key Parameter File containing the velocity profiles, error estimates, and

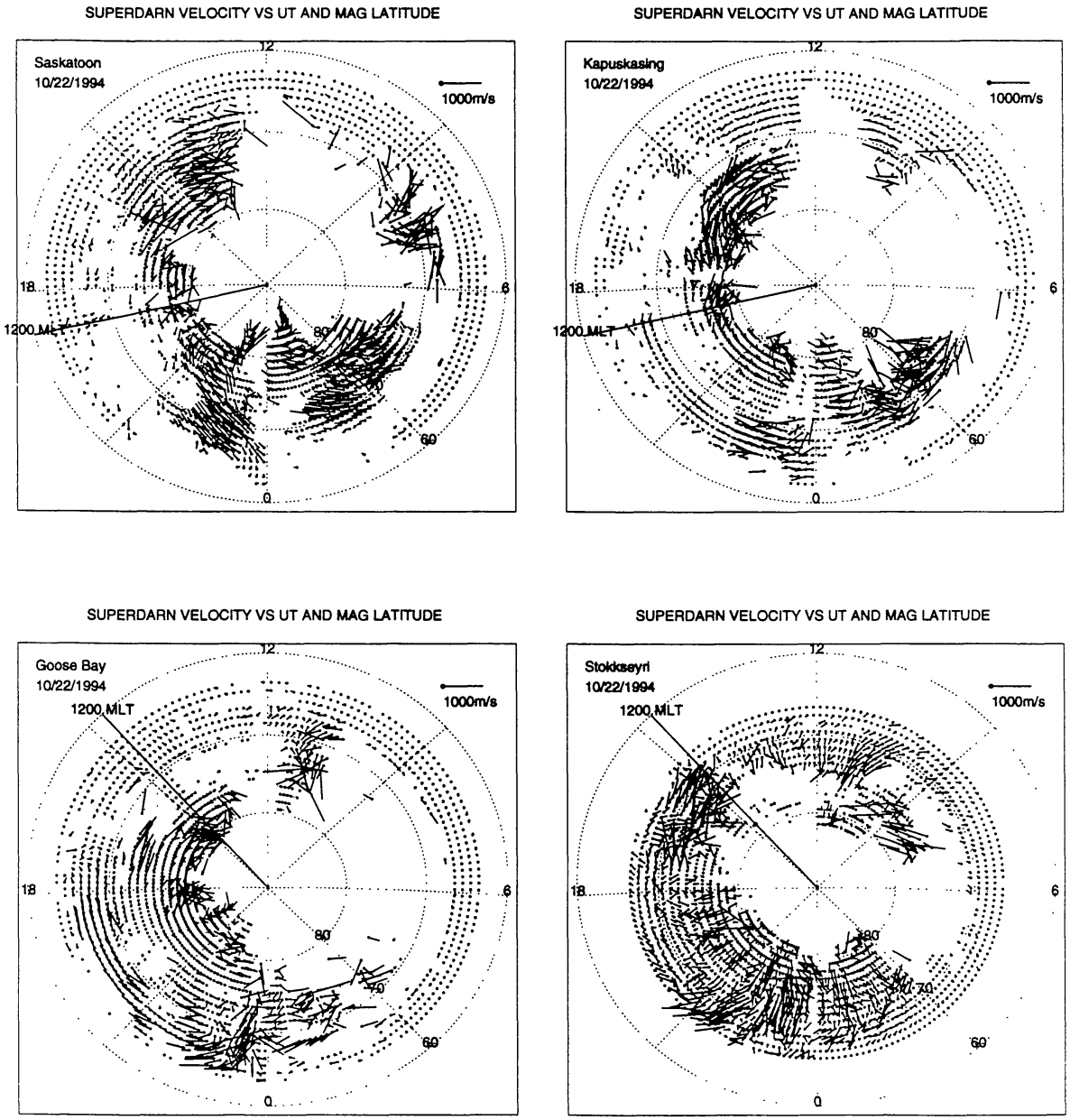

Fig. 18. Clock-dial plots of Key Parameter data from the northern-hemisphere Saskatoon, Kapuskasing, Goose Bay, and Stokkseyri radars. These data are currently being submitted to the ISTP/GGS Central Data Handling Facility on a daily basis. Each plot displays velocity vectors derived from the scanned Doppler data of that radar using the technique developed by Ruohoniemi *et al.* (1989). The data are plotted in universal time with the nominal noon magnetic meridian indicated. No vector is plotted if the Doppler data do not exhibit sufficient sinusoidal variability during the azimuth scan. Similar data are also being submitted daily from the HF radar located at Halley Station, Antarctica.

flags indicating how the vectors were determined, will then be submitted to the CDHF.

Some software has been developed at JHU/APL to take this Key Parameter data and produce clockdial plots of ionospheric echo occurrence and vector velocity. Figure 18 shows an example of each of these plots with the velocity information having been averaged over 2° in latitude and 10 min in Universal Time.

The SuperDARN investigators have identified three categories of radar operation:

Common Programs: Several standard operating modes of the radars for which all radars will be operated in the same manner. Common programs will comprise 50% of the total operation. Data from this type of operation will be available for Key Parameters and ISTP Event Studies.

SuperDARN Special Programs: Special operating modes agreed upon by the PIs for the purpose of achieving specific research goals. Special programs will be limited to 20% of the total operation. Data from this type of operation will be available for Key Parameters and ISTP Event Studies.

Discretionary Operations: Operations set aside for the PIs to pursue personal or collaborative research goals. Discretionary time will be limited to 30% of the radar operations. Data from this type of operation will be available only at the discretion of the individual PIs. PIs not participating in a discretionary study may operate their radar in a Common Program or SuperDARN Special Program format.

All time not used under Discretionay Operations or SuperDARN Special Program operation will revert to Common Program time.

4. Summary

The DARN investigation team is actively deploying extended longitudinal arrays of SuperDARN HF radar pairs and awaiting the renewed operation of the upgraded STARE radar system. We believe that the global character of these radar observations will provide considerable new insight into the electrodynamic nature of many large-scale magnetospheric processes. Since the data sets from the various radar

elements are inherently the same and since they are designed to be analyzed together, we believe that global-scale DARN/SuperDARN analyses will be performed with an ease that has not yet been possible with ground-based data.

The DARN investigation team is looking forward to successful launches of all ISTP-related spacecraft that will be in orbit during the time frame of the ISTP/GGS study and to the subsequent launch of CLUSTER. We believe that measurements obtained with DARN will be a valuable contribution to collaborative studies with experiments on any and all of these spacecraft.

Acknowledgements

This work was prepared under support of NASA Grant NAG5-1099. The radars of the DARN experiment operate under the sponsoring agencies credited previously in this paper.

References

Aarons, J.: 1973, *J. Geophys. Res.* **78**, 7441.
Baker, K.B., Greenwald, R.A., Rouhoniemi, J.M., Dudeney, J.R., Pinnock, M., and Mattin, N.: 1989, *Eos Trans. AGU* **70**(34), 785.
Bristow, W.A., Greenwald, R.A., and Samson, J.M.: 1993, *J. Geophys. Res.*, in press.
Buneman, O.: 1963, *Phys. Rev. Letts.* **10**, 285.
Burke, W.J., Kelley, M.C., Sagalyn, R.C., Smiddy, M., and Lai, S.T.: 1979, *Geophys. Res. Letts.* **6**, 21.
Cahill, R.A., Greenwald, R.A., and Nielsen, E.: 1978, *Geophys. Res. Letts.* **5**, 687.
de la Beaujardiere, O., Alcayde, D., Fontanari, J., and Leger, C.: 1991, *J. Geophys. Res.* **96**, 5723.
Dudeney, J.R., Rodger, A.S., Pinnock, M., Ruohoniemi, J.M., Baker, K.B., and Greenwald, R.A.: 1991, *J. Atmos. Terr. Phys.* **53**, 249.
Dungey, J.W.: 1956, *J. Atmos. Terr. Res.* **9**, 304.
Farley, D.T.: 1963, *J. Geophys. Res.* **68**, 6083.
Fejer, B.G., and Kelley, M.C.: 1980, *Rev. of Geophys. and Space Phys.* **18**, 401.
Fejer, B.G., Reed, R.W., Farley, D.T., Swartz, W.E., and Kelley, M.C.: 1984, *J. Geophys. Res.* **89**, 187.
Foster, J.C.: 1983, *J. Geophys. Res.* **88**, 981.
Freeman, M.P., Ruohoniemi, J.M., and Greenwald, R.A.: 1991, *J. Geophys. Res.* **96,** 15, 735.
Greenwald, R.A., Ecklund, W.L., and Balsley, B.B.: 1975, *J. Geophys. Res.* **80**, 3635.
Greenwald, R.A., Weiss, W., Nielsen, E., Thomson, N.R.: 1978, *Radio Sci.* **13**, 1021.
Greenwald, R.A., and Walker, A.D.M.: 1980, *Geophys. Res.Letts.* **7**, 745.
Greenwald, R.A., Baker, K.B., and Villain, J.-P.: 1983, *Radio Sci.* **18**, 1122.
Greenwald, R.A., Baker, K.B., Hutchins, R.A., and Hanuise, C.: 1985, *Radio Sci.* **20**, 63.
Greenwald, R.A., Baker, K.B., Ruohoniemi, J.M., Dudeney, J.R., Pinnock, M., Mattin, N., Leonard, J.M., and Lepping, R.P.: 1990, *J. Geophys. Res.* **95,** 8057.
Haldoupis, C., Schlegel, K., and Nielsen, E.: 1993, *Annales Geophys.* **11**, 283.
Hanuise, C., Villain, J.-P., Crochet, M.: 1981, *Geophys. Res. Letts.* **8**, 1083.
Hanuise, C., Senior, C., Cerisier, J.-C., Villain, J.-P., Greenwald, R.A., Ruohoniemi, J.M., and Baker, K.B.: 1993, *J. Geophys. Res.* **98**, 17387.
Heelis, R.A.: 1984, *J. Geophys. Res.***89**, 2873.
Heppner, J.P., and Maynard, N.C.: 1987, *J. Geophys. Res.* **92**, 4467.
Inhester, B., Baumjohann, W., Greenwald, R.A., and Nielsen, E.: 1981, *J. Geophys.* **49**, 155.

Keskinen, M.J., Mitchell, H.G., Fedder, J.A., Satuanarayana, P., Zalesak, S.T., and Huba, J.D.: 1988, *J. Geophys. Res.* **93**, 137.
Knox, F.B.: 1964, *J. Atmos. Terr. Phys.***26**, 239.
Kueppers, F., Untiedt, J., Baumjohann, W., Lange, K., and Jones, A.G.: 1979, *J. Geophys.* **46**, 429.
Kunkel, T., Baumjohann, W., Untiedt, J., and Greenwald, R.A.: 1986, *J. Geophys.* **59**, 73.
McNamara, A.G., McDiarmis, D.R., Sofko, G.J., Koehler, J.A., Forsyth, P.A., and Moorcroft, D.R.: 1983, *Adv. Space Res.* **2**, 145.
Nielsen, E., and Greenwald, R.A.: 1979, *J. Geophys. Res.* **84**, 4189.
Nielsen, E. and Schlegel, K.: 1983, *J. Geophys. Res.* **88**, 5745.
Nielsen, E., W. Guettler, E.C. Thomas, C.P. Stewart, T.B. Jones and A. Hedberg, 1983, *Nature* **304**, 712.
Nielsen, E., and Schlegel, K.: 1985, *J. Geophys. Res.* **90**, 3498.
Ossakow, S.L., and Chaturvedi, P.K.: 1979, *Geophys. Res. Letts.* **6**, 332.
Pinnock, M., Rodger, A.S., Dudeney, J.R., Baker, K.B., Newell, P.T., Greenwald, R.A., Greenspan, M.E.: 1993, *J. Geophys. Res.* **98**, 3767.
Reid, G.C.: 1968, *J. Geophys. Res.* **73,** 1627.
Richmond, A.D. and Y. Kamide, 1988, *J. Geophys. Res.* **93**, 5741.
Robinson, T.R.: 1994, *Annales Geophys.*, in press.
Ruohoniemi, J.M., Greenwald, R.A., Baker, K.B., Villain, J.-P., and McCready, M.A.: 1987, *J. Geophys. Res.* **92**, 4553.
Ruohoniemi, J.M., Greenwald, R.A., Villain, J.-P., Baker, K.B., Newell, P.T., and Meng, C.-I.: 1988, *J. Geophys. Res.* **93**, 12,871.
Ruohoniemi, J.M., Greenwald, R.A., Baker, K.B., Villain, J.-P., Hanuise, C., and Kelly, J.: 1989, *J. Geophys. Res.* **13**, 463.
Samson, J.C., Greenwald, R.A., Ruohoniemi, J.M., Frey, A., and Baker, K.B.: 1990, *J. Geophys. Res.* **95**, 7693.
Senior, C., Fontaine, D., Caudel, G., Alcayde, D., Fontanari, J.: 1990, *Annales Geophysicae* **8**, 257.
Simon, A.: 1963, *Phys. Fluids* **15**, 1507.
Tsunoda, R.T., Barons, M.J., Owen, J., and Towle, D.M.: 1979, *Radio Sci.* **14**, 1111.
Villain, J.-P., Caudal, G., Hanuise, C.: 1985, *J. Geophys. Res.* **90**, 8433.
Waldock, J.A., Jones, T.B., and Nielsen, E.: 1985, *Nature* **313**, 204.
Walker, A.D.M., Greenwald, R.A., Stuart, W.F., and Green, C.A.: 1979, *J. Geophys. Res.* **84**, 3373.
Woodman, R.F., and La Hoz, C.: 1976, *J. Geophys. Res.* **81**, 5447.